Met O 19 Branch Memorandum No. 49

OBSERVATIONS OF THE STRATOSPHERIC AEROSOL LAYER MADE WITH THE BEAUFORT PARK LIDAR

by

J.I. GIBBS

Met O 19
High Atmosphere Branch
Meteorological Office
London Road
BRACKNELL
Berkshire RG12 2SZ

April 1979

Observations of the stratospheric aerosol layer made with the Beaufort Park Lidar

by J. I. Gibbs

1. Introduction

The Beaufort Park Lidar, which was designed to detect the backscatter at a wavelength corresponding to the Raman shift by molecular nitrogen relative to the dye laser pulse, has been described by Pettifer et al (1976). As measurements of the Raman-shifted signal became available it was apparent that large statistical errors in the measurement of temperature at high altitudes, due to the very small return signal, made the data far less valuable, from the meteorological point of view, than temperatures derived from the rapidly developing technique of satellite radiometry. For this reason no further experiments of this type were carried out beyond March 1974.

Having proved the lidar system inadequate for temperature measurements alternative applications were considered. The installation in its existing form was shown to be capable of measuring elastically backscattered radiation from aerosol in the stratosphere as well as detecting high level cloud (Jenkins and Healey, 1979), and the Beaufort Park lidar has been used for these purposes since mid-1974. This programme has been handicapped by weather conditions and the characteristics of the lidar, which together severely restricted the number of observations. Whilst minor modifications of the system to optimize it for these studies would undoubtedly make more frequent observations possible, the difficulties of interpreting any lidar observations in terms of radiative effects in the stratosphere (highlighted by Slingo et al, 1977) would remain. Since such observations are no longer unique, it has been decided that the effort needed to operate the system cannot be justified. The last observations were made in January 1978 and were followed by a study evaluating the lidar.

The purpose of this report is to put on record the measurements of stratospheric aerosol made during this programme, defining the techniques of observations and data reduction used. It will be assumed that readers are familiar with the basic theory of lidar and the original form of the Beaufort Park lidar. Suitable accounts can be found in Slingo et al (1977) and Pettifer et al (1976).

2. Description of Equipment

The original system has been described by Pettifer et al (1976). During the period since then, the equipment has remained unaltered. The only change made has been in the operating voltage of the photomultiplier tube. This was reduced, from 2.0 kV to 1.7 kV, to minimize the effects of signal induced noise. For a full discussion of this phenomenon see Pettifer et al (1974).

The system (Fig. 22) was based upon a large flash-lamp pumped organic dye laser. This gave a 2 joule output at 605 nm using Rhodamine 6G and 1 joule at 465 nm using esculin monohydrate. The laser was capable of a pulse repetition frequency of one shot per second. The pulse width varied but was generally between 4 to 6 μs at full width half maximum.

Although the backscatter return (proportional to $1/\lambda^4$) for esculin monohydrate more than compensated for its smaller energy output, the dye suffered from photodegradation more severely than Rhodamine 6G resulting in a rapid fall-off in pulse energy. Furthermore esculin monohydrate could only be dissolved completely in a pure ethanol solution which after use required distillation, to extract the ethanol. For these reasons most of the observations were made using Rhodamine 6G, which was dissolved in a mixture of distilled water and ethanol which was disposed of after use.

For aerosol studies one needs to measure the backscattering profile upwards from 10 km. The elastically backscattered signal from around 10 km is very large and the count rates experienced by the photon counters are large enough for pulse pile-up errors to become significant. These errors occur because of the finite 'dead-time' of the counters (τ = 28 ns). When the probability of more than one pulse arriving during the time τ is negligible, the true count rate N_T is given by the simple relation

$$N_T = N_A/(1 - \tau N_A) \qquad (2.1)$$

where N_A is the measured count rate (Pettifer, 1975).

Equation 2.1 is invalid for count rates such that $(N_T-N_A)/N_A > 0.3$. In practical terms this means that the number of counts for 2 km range bins must not exceed 100 per laser shot. This condition is realised by placing neutral density filters between the main mirror and the diaphragm (Fig. 22).

3. Method of Analysis

A detailed account of the basic lidar theory has been given by Pettifer (1975) and a further analysis of the effects of the underlying assumptions, experimental errors and uncertainties in aerosol physical properties was provided by Slingo et al (1977). Consequently this section concentrates on defining the data reduction techniques which we have used, including a description of a correction applied for the finite width of the laser pulse.

Pulses, each representing the emission of a single photoelectron from the cathode of the photomultiplier, were directed to one of a series of 19 counters according to their delay with respect to the laser output pulse. The counts accumulated in the counters corresponded to the backscattered return from consecutive layers of the atmosphere. Each such layer was 2 km thick and, for most of the observations, the lowest layer was centred at 11 km, the highest at 37 km.

For such a system the photon count n at each level is subject to an uncertainty of $\sqrt{n}$. As a target we aimed to reduce this random error, allowing for photo-multiplier dark-current, to below 3 per cent at the highest level at which radiosonde comparison data was available. In practice this meant continuing laser firings until about 1000 counts were recorded at the highest level of normalisation (usually 31 km) which overlaps the top of the radiosonde ascent.

The radiosonde ascent is used to compute an air density profile from which the backscatter profile due to air molecules can be calculated. In order to ensure that this calculated backscatter profile is a good approximation to the air mass over

Beaufort Park the Crawley midnight radiosonde ascent, corresponding to the date of a backscatter measurement, is used for these air density calculations.

Corrections were applied to take into account attenuation of the beam due to both the atmosphere and ozone. For a complete account of the theory of aerosol backscatter investigations, including the so-called clean air normalisation technique, see Pettifer (1975). In this report a brief outline of the technique is given below.

It has been shown by Kent et al (1967) that the number of backscattered photons received from a layer of air, thickness δz at altitude z, from a single pulse is given by,

$$P(z) = \frac{P_0 E q_0^2 q^2(z) \delta z (f_p + f_m)}{z^2} \quad (3.1)$$

(see table 2 for key to symbols).

The backscattered signal from air molecules alone is given by

$$M(z) = \frac{P_0 E q_0^2 q^2(z) \delta z f_m}{z^2} \quad (3.2)$$

Dividing 3.1 by 3.2 gives

$$R(z) = \frac{P(z)}{M(z)} = 1 + \frac{f_p}{f_m} \quad (3.3)$$

From equn 3.3 it can be seen that for aerosol free air (ie 'clean' air) for which f_p is zero, the ratio $R(z)$ is unity.

Because of the difficulties associated with measuring quantities such as E, the receiver efficiency, and P_0 the number of photons in the lidar pulse, it is necessary to analyse the lidar data on the assumption that there sits a clean air layer somewhere within the height range of the backscatter ratio measurements.

Atmospheric levels (z') centred on each 2 km range bin in turn were assigned as the normalisation level and a series of profiles of $R(z)$ were plotted for each such level. These profiles were examined and the one for which all values of $R(z)$ were greater than or equal to unity selected as representing the backscatter profile. Data below 11 km was not used because of the possibility of the presence of cirrus cloud, and data above 33 km was ignored because of the large error bars associated with it.

It was observed, on the backscatter profiles, that unexpectedly large values of backscatter ratio $R(z)$ were recorded at low levels (7 to 11 km). The variation with altitude was smooth, with no suggestion of the layered structure to be expected from cirrus cloud. The anomalously large value of $R(z)$ at low levels (below 13 km) has been traced to an error in the assigned time of the laser pulse. The timing of a pulse was measured from its leading edge. Subsequent calculations of height, determined from the time taken for the return signal to reach the appropriate counter, are based on this assumption. Thus, if t_0 is the time at the start of an ideal very narrow laser pulse and t_1 is the time taken for that pulse to reach the base of the required atmospheric layer, then backscattered photons from that level will start arriving at the receiver at $t_0 + 2t_1$. The appropriate counter is held open for an interval 2Δ, where Δ is the depth (expressed in time of travel) of the layer. However, if the laser pulse has a width t_2 then photons accepted by the counter may have had travel times between $2t_1 - t_2$ and $2t_1 + 2\Delta$. Thus the depth of the layer from which the echo is detected is increased, from Δ to $\Delta + 0.5t_2$, the lower boundary is decreased by the layer equivalent of $0.5t_2$ and the mean height, z, correspondingly decreased. Since the signal received is proportional to $1/z^2$ any such offset error in z will cause an increasing departure in received signal as z decreases. The calculation of a precise correction factor for the finite width of the pulse would require deconvolving the laser pulse profile with the backscatter profile. Because the variability of the output pulse shape over the period of a run was not known this technique was not used. A simple correction was applied which considered the centre of the pulse (ie the 50 per cent energy release) to be the reference for timing purposes. This reduction was sufficient to reduce the aerosol backscatter ratio at lower levels to values approaching unity in the absence of cirrus cloud.

The timing error discussed above can be made negligibly small if the laser pulse width is much less than the width of the range bin. It was not possible to effect a significant decrease in the pulse width of the double elliptical cavity (DEC) laser without major modifications to the charge-discharge circuitry. An alternative approach was to adopt a laser with a much smaller pulse width. The laser based on the COX-3 coaxial flash tube (Morrow and Price, 1974) was selected for this purpose, and some studies of the COX-3 are described in Appendix 1.

For a complete account of the errors introduced by the 'clean-air' calibration, atmospheric transmission, pulse counting errors etc see Slingo et al (1977).

4. Discussion of Results

In the three year period during which backscatter profiles were measured 18 satisfactory runs were completed at 605 nm. The successful runs covered the period from July 1976 to January 1978. Prior to this (ie between March 1974 and July 1976) several backscatter experiments were carried out. However, the data analysis and format for these differ from those presented in this report. The basic data that would enable an analysis for this earlier period is not available. Consequently the output has been archived together with the analysed data but not in the same form.

The backscatter ratio profiles for the 18 satisfactory runs are shown in Figs 1 to 18. Each of these profiles was obtained over a period of four to five hours at night and where possible centred on midnight. It can be seen that, on the 2 km vertical resolution scale, the profiles exhibit structure in the form of maxima and minima in aerosol backscatter ratio which, it is assumed, reflect the vertical concentration of aerosol. The lowest layer has a maximum which varies in altitude between 16.5 and 20.5 km (see Table 1). It thus corresponds with the well documented Junge layer. The higher altitude layers appear as separate entities but there is little consistency in their height on any but a short time scale. For example Figs 1 to 5 cover a period of 52 days during which time a prominent layer at about 26.5 km was present. A further layer is present occasionally at 30.5 km. The range of the profiles presented in Figs 1 to 18 is from 14.5 km to 32.5 km. Data is available on the computer printout sheets for heights above and below these limits, but is not presented in this report. The lower level data is suspect as anomalously large backscatter ratios are occasionally recorded, presumably due to the presence of cirrus cloud. At levels above 32.5 km the error bars on the data become too large to justify plotting the values. Inaccurate shutter timing occasionally produces less than unity ratios at the 11-13 km levels.

Two dual wavelength Rayleigh runs have been carried out. The results of the first run, on 12/13 January 1975, are described in Pettifer et al (1976). The second experiment was carried out on 23/24 May 1977 and the results are displayed in Fig 19. These experiments were carried out in the hope of eliminating the need for the so-called clean air assumption. For a critique of this type of experiment see Slingo et al (1977).

The mean backscatter ratio profile for 1977 (nine profiles) is presented in Fig 20. A maximum in aerosol scattering is observed at 20.5 km which is in good agreement with the reported height of the Junge layer as measured by other techniques. The higher level layers are not apparent on this profile, being masked by their variability.

An analysis was carried out to determine the effects of selecting different normalisation levels on the shape of the backscatter profiles. Fig 21 shows the result of normalizing the mean 1977 profile at the high and low levels commonly used. Scattering ratios derived with a normalisation level of 31 km are plotted against those derived with an 11 km normalisation level. It can be seen that the choice of normalisation level results in an error in scattering ratio of between 5 and 8 per cent over the altitude range.

Because of the paucity of observations, due mainly to climatological conditions, difficulties were encountered in carrying out a time series analysis of the data. It was not possible to follow the variation in aerosol structure on a short enough time scale (ie 1 to 2 days) to examine the effects of volcanic activity or other sources of aerosol on the stratospheric aerosol loading.

Fig 23-24 represent an attempt to present all the data bearing in mind the above limitation. Fig 23 shows the average backscatter ratio, $R(z)$, over the height range 13 to 33 km. Fig 24 shows the relative contributions of the excess scattering $[R(z)-1]$ from the layers 15-23 km and 23-33 km respectively. It can be seen from the scatter of the points that, even with this coarse comparison, no real conclusions can be made with regard to the temporal variability of the aerosol.

A catalogue of all the data for vertical profiles has been compiled. It consists of the computer printouts of the supplementary data (eg Crawley radiosonde ascents) together with a succession of backscatter profiles normalised at 2 km intervals up to 31 km. This catalogue is lodged in the Meteorological Office archives and is referenced as Met O 19 Item No 19 entitled "Lidar investigations of stratospheric aerosol: data and results".

5. Conclusions

The lidar installation at Beaufort Park has proved to be a reliable and effective instrument in its limited role of studying the stratospheric aerosol backscatter ratio.

The principle limitations, which resulted in the cessation of the project, were:

a. Due to climatological conditions at Beaufort Park there were too few days during a year when observations could be made.

b. As a consequence of a. it has not proved possible to study the effects of volcanic eruptions, meteor showers etc, on the vertical distribution of aerosol.

c. Modifications to the existing system either to minimize the impact of cloud on aerosol studies or to enable its use in an alternative role (ie cirrus cloud studies) was not considered cost-effective. An account of the most important possible modification, involving the use of a co-axial dye laser, is given in the Appendix.

References

1. Pettifer, R. E. W., Jenkins, G. J., Healey, P. G., and Convery, J. H. Optical and Quantum Electronics 8, (1976), 409-423.
2. Jenkins, G. J., Healey, P. G. Private communication (1979).
3. Slingo, A., Jenkins, G. J., and Hunt G. E., Met O 19 Branch Memorandum No 38, (1977).
4. Pettifer, R. E. W. and Healey P. G., J. Phys. E 7, (1974) 617-620.
5. Pettifer, R. E. W. PhD Thesis, Queens University of Belfast, (1975).
6. Kent, G. S., Clemesha, B. R. and Wright, R. H. W. J. Atm. Terr. Phys. 29, (1967), 169-181.

FIG NO	DATE	HEIGHTS OF MAXIMA (KM)			WAVELENGTH (nm)
1	29/30.7.76	18.5	26.5	30.5	605
2	15/16.8.76	18.5	28.5		"
3	16/17.8.76	16.5	26.5		"
4	23/24.8.76	18.5	26.5	30.5	"
5	18/19.9.76	18.5	26.5		"
6	2/3.11.76	22.5	30.5		"
7	3/4.11.76		26.5	30.5	"
8	2/3.12.77	18.5	22.5	30.5	"
9	11/12.2.77	16.5	20.5	26.5	"
10	7/8.3.77	22.5	26.5	30.5	"
11	31 MAR/1 APR 77	19-21	24.5	30.5	"
12	25/26.4.77	20.5			"
13	18/19.5.77	20.5			"
14	23/24.5.77	16.5	20.5	22.5	"
15	1/2.8.77	18.5	28.5		"
16	10/11.8.77	18.5-20.5	28.5		"
17	13/14.9.77	20.5-22.5		30.5	"
18	26/27.1.78	20.5		30.5	"
19	23/24.5.77	22.5	28.5		465
		16.5	20.5	22.5	605

TABLE 1. HEIGHTS OF AEROSOL MAXIMA

Table 2

Definition of symbols used in Section 3

z	altitude variable
δz	altitude increment (or layer)
z'	altitude at which aerosol assumed to be absent
z_1	lowest altitude at which lidar signal analysed
E	receiver system efficiency
q_o	atmospheric transmission between ground and z_1
$q(z)$	atmospheric transmission between z_1 and z
P_o	number of photons transmitted
$P(z)$	number of photons received from altitude z
f_m	molecular backscatter coefficient
f_p	aerosol backscatter coefficient
$R(z)$	scattering ratio at altitude z
R_{max}	maximum value of $R(z)$ in a profile

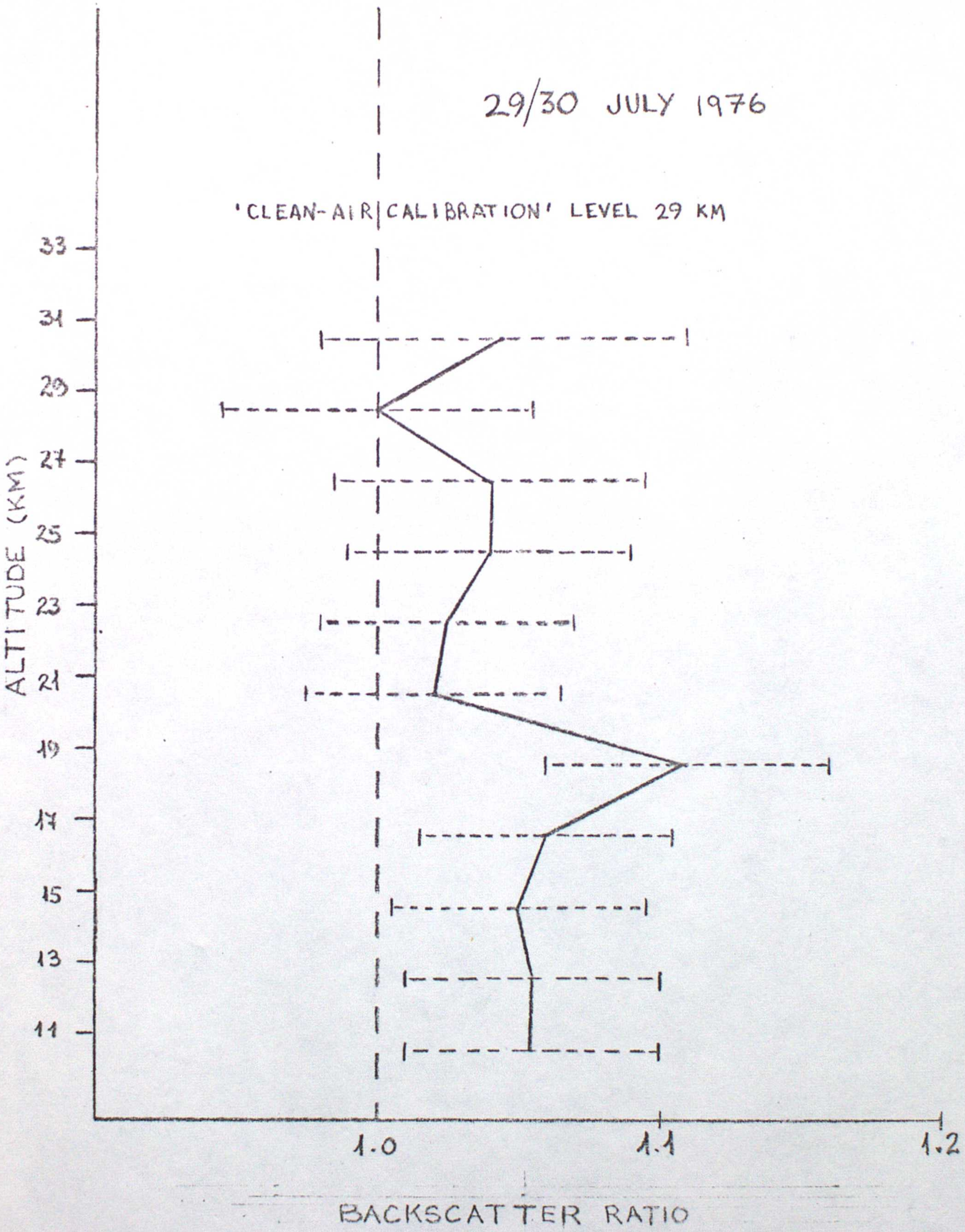
29/30 JULY 1976
'CLEAN-AIR CALIBRATION' LEVEL 29 KM
ALTITUDE (KM)
33
31
29
27
25
23
21
19
17
15
13
11
1.0
1.1
1.2
BACKSCATTER RATIO

FIG. 1

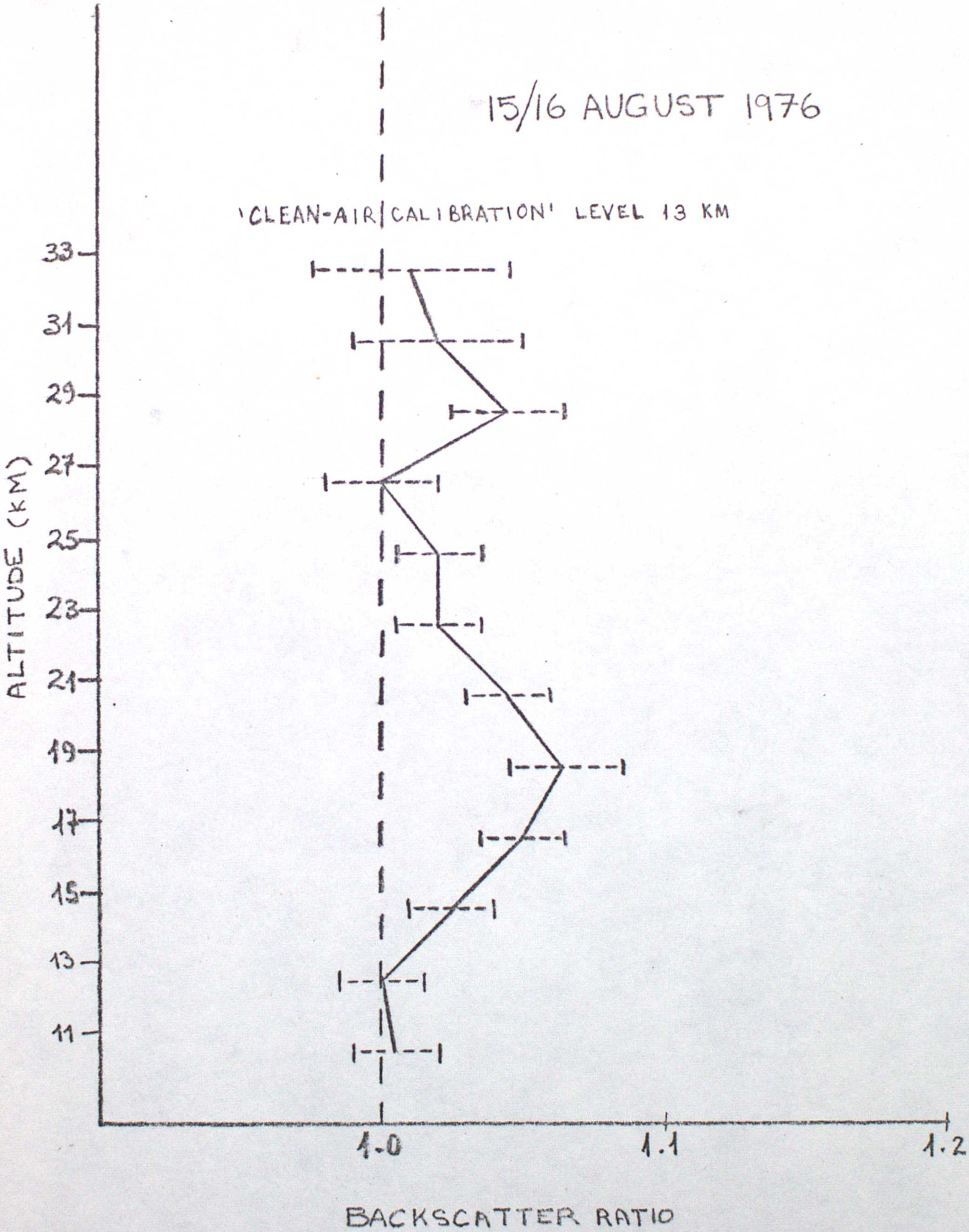

15/16 AUGUST 1976
'CLEAN-AIR CALIBRATION' LEVEL 13 KM
ALTITUDE (KM)
33
31
29
27
25
23
21
19
17
15
13
11
1.0
1.1
1.2
BACKSCATTER RATIO

FIG. 2

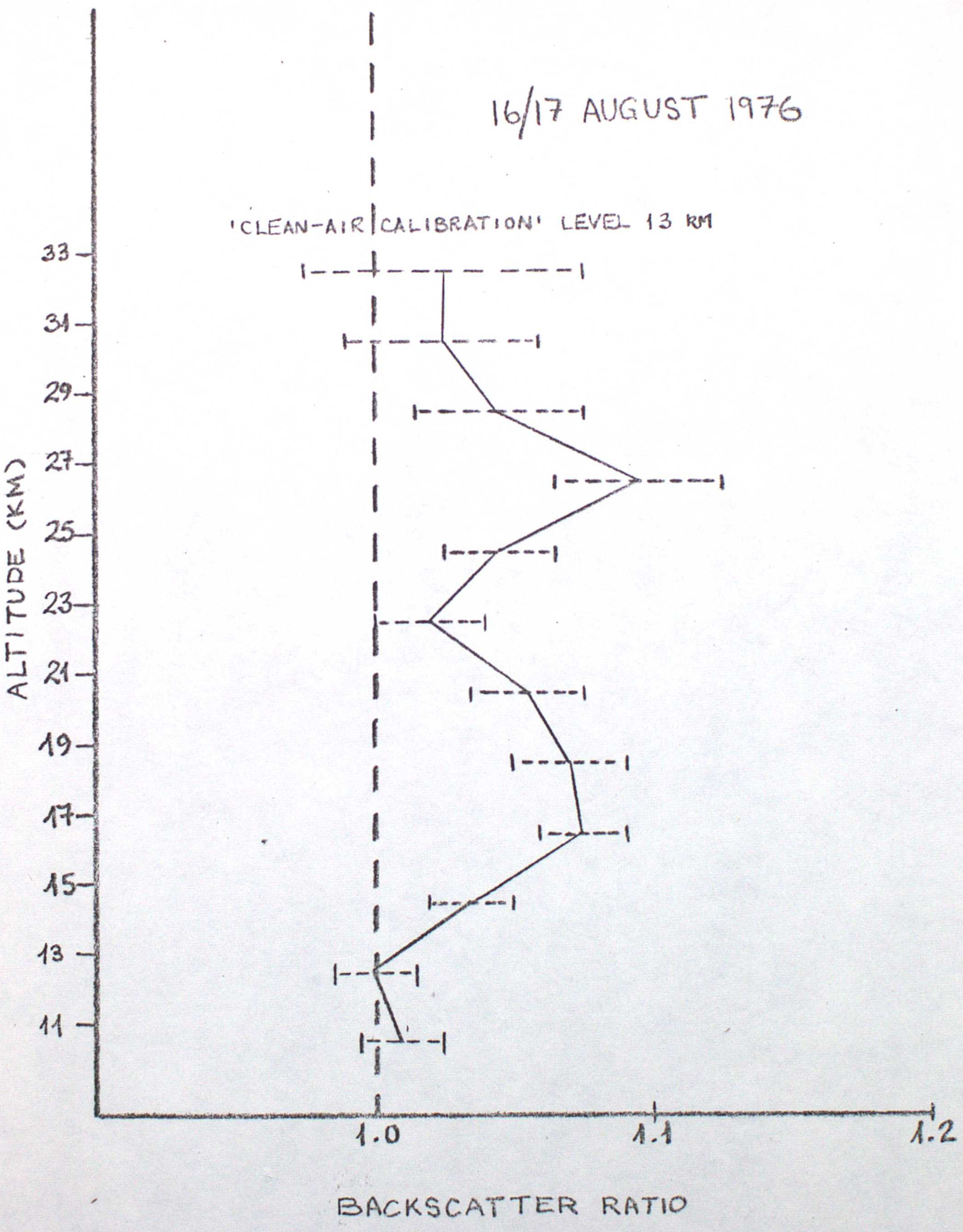
16/17 AUGUST 1976
'CLEAN-AIR CALIBRATION' LEVEL 13 KM
ALTITUDE (KM)
33
31
29
27
25
23
21
19
17
15
13
11
1.0
1.1
1.2
BACKSCATTER RATIO

FIG. 3

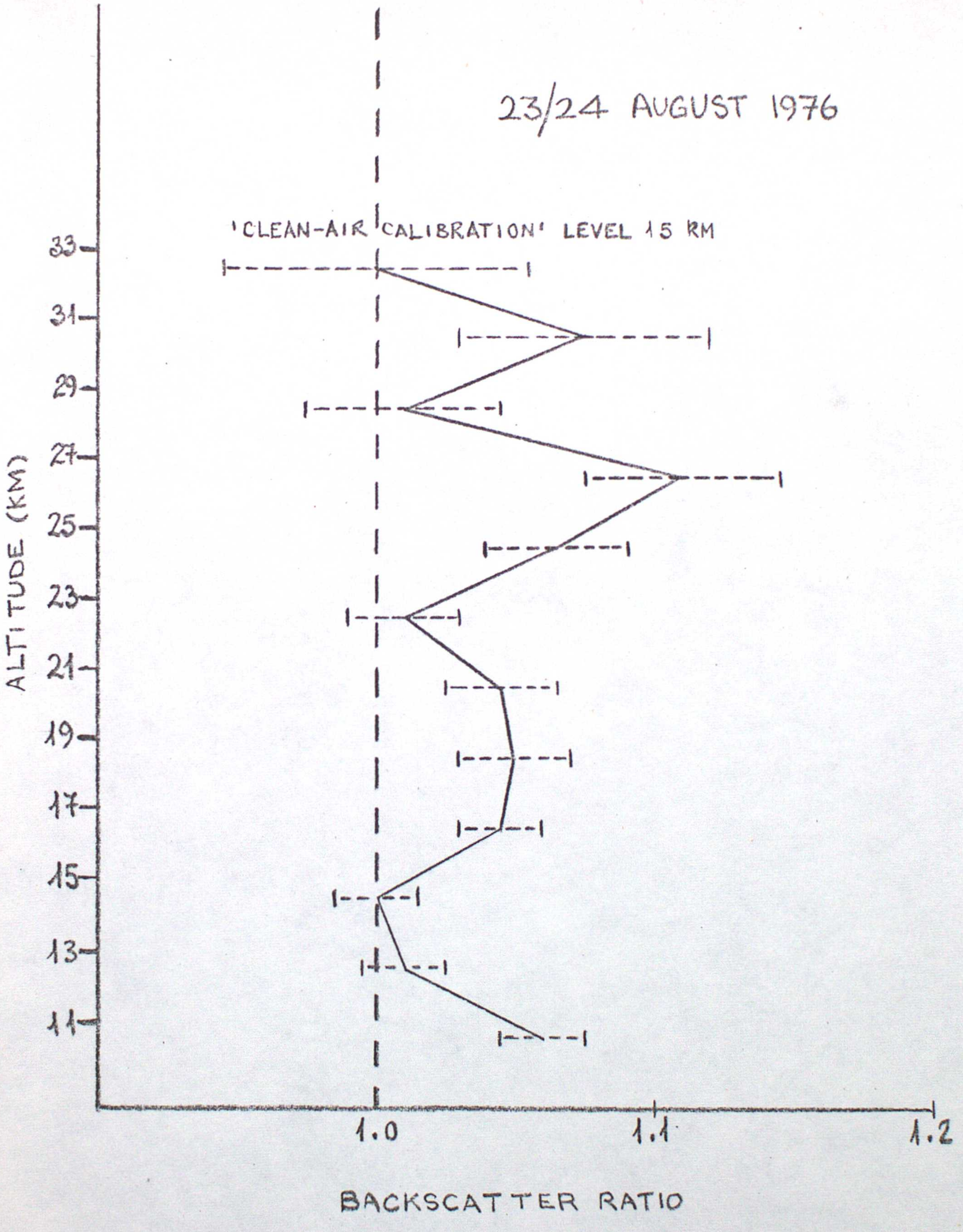
23/24 AUGUST 1976
'CLEAN-AIR CALIBRATION' LEVEL 15 KM
ALTITUDE (KM)
33
31
29
27
25
23
21
19
17
15
13
11
1.0
1.1
1.2
BACKSCATTER RATIO

FIG. 4

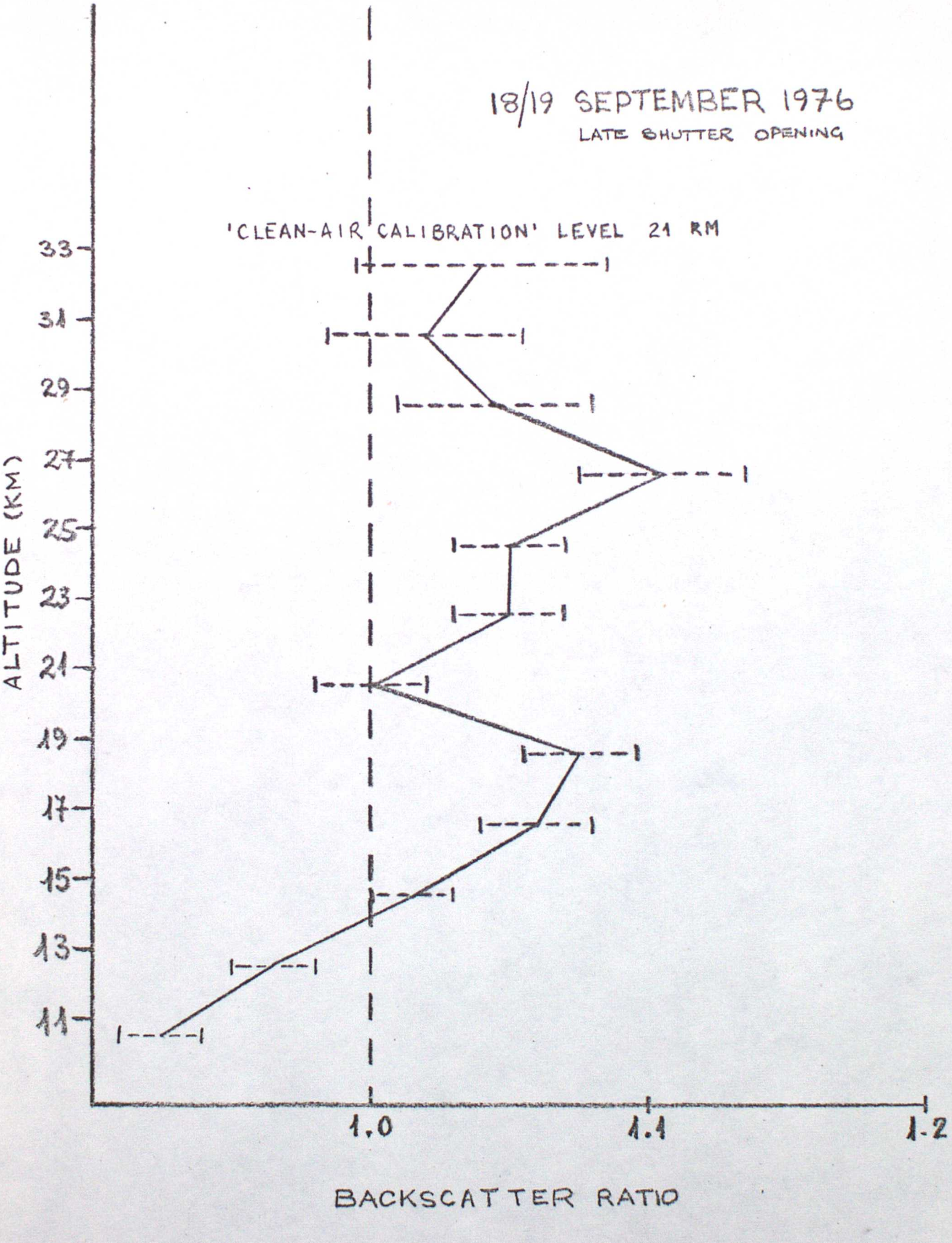
18/19 SEPTEMBER 1976
LATE SHUTTER OPENING
'CLEAN-AIR CALIBRATION' LEVEL 21 KM
ALTITUDE (KM)
33
31
29
27
25
23
21
19
17
15
13
11
1.0
1.1
1.2
BACKSCATTER RATIO

FIG. 5

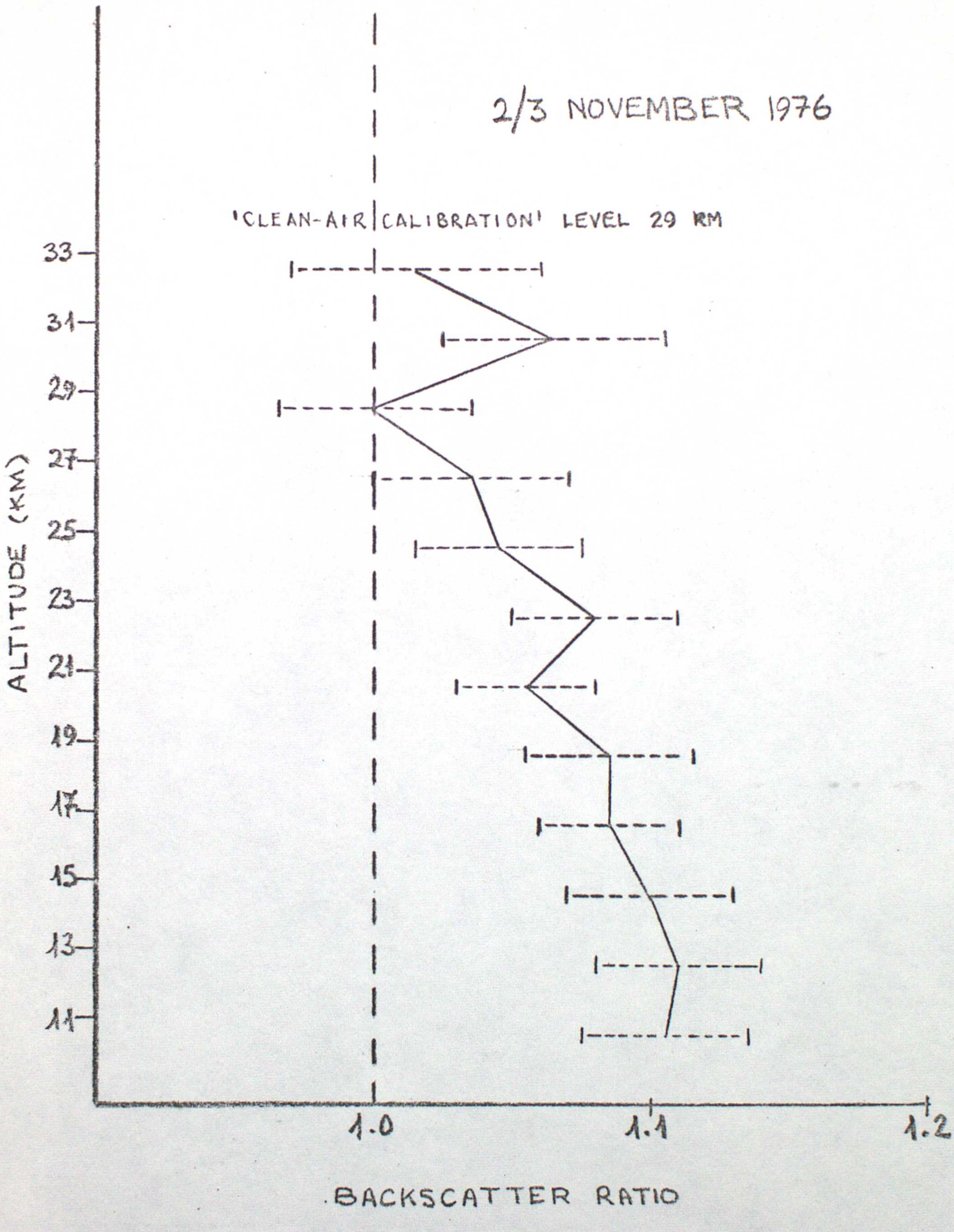
2/3 NOVEMBER 1976
'CLEAN-AIR CALIBRATION' LEVEL 29 KM
33
31
29
27
25
23
21
19
17
15
13
11
ALTITUDE (KM)
1.0
1.1
1.2
BACKSCATTER RATIO

FIG. 6

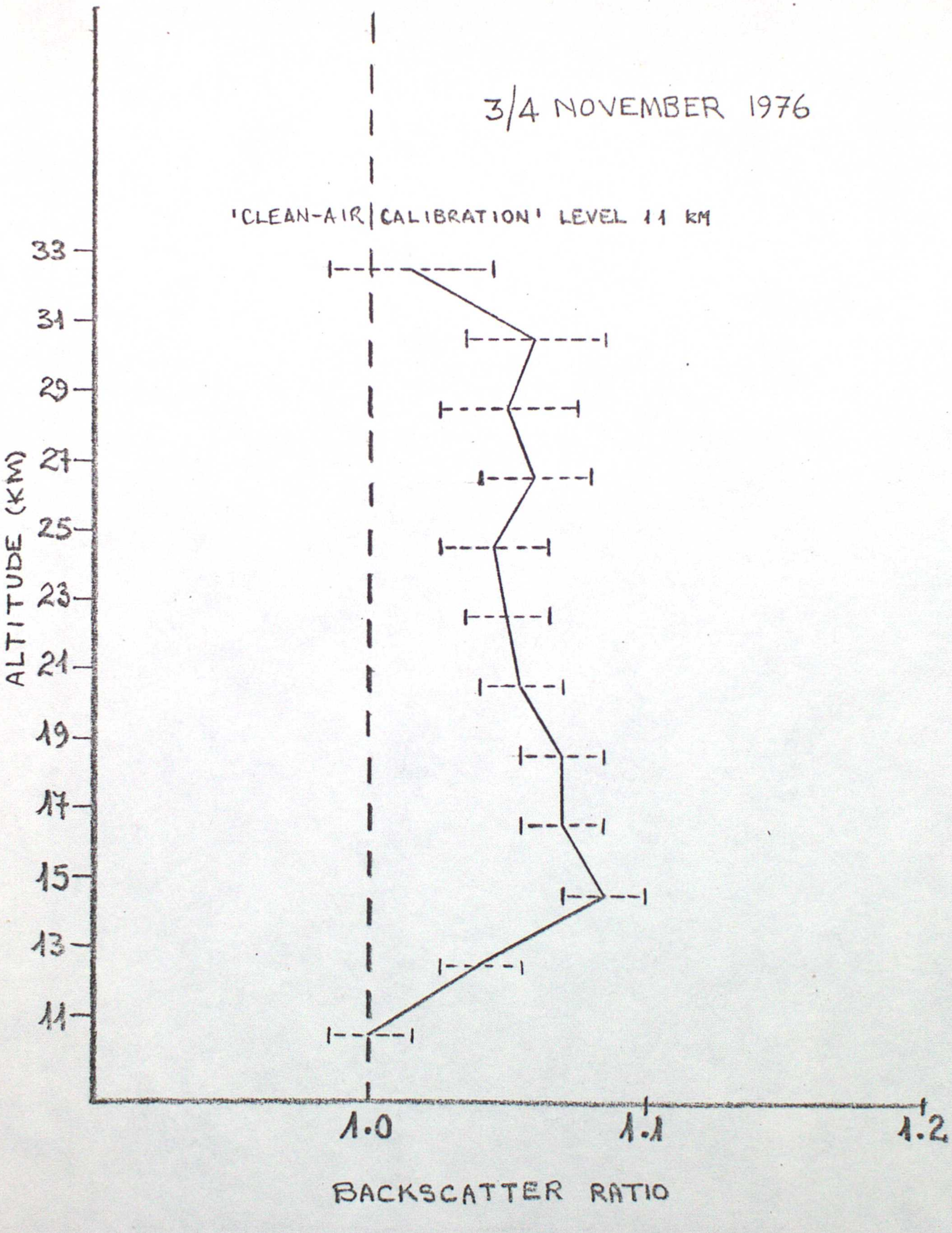
3/4 NOVEMBER 1976
'CLEAN-AIR CALIBRATION' LEVEL 11 KM
ALTITUDE (KM)
33
31
29
27
25
23
21
19
17
15
13
11
1.0
1.1
1.2
BACKSCATTER RATIO

FIG. 7

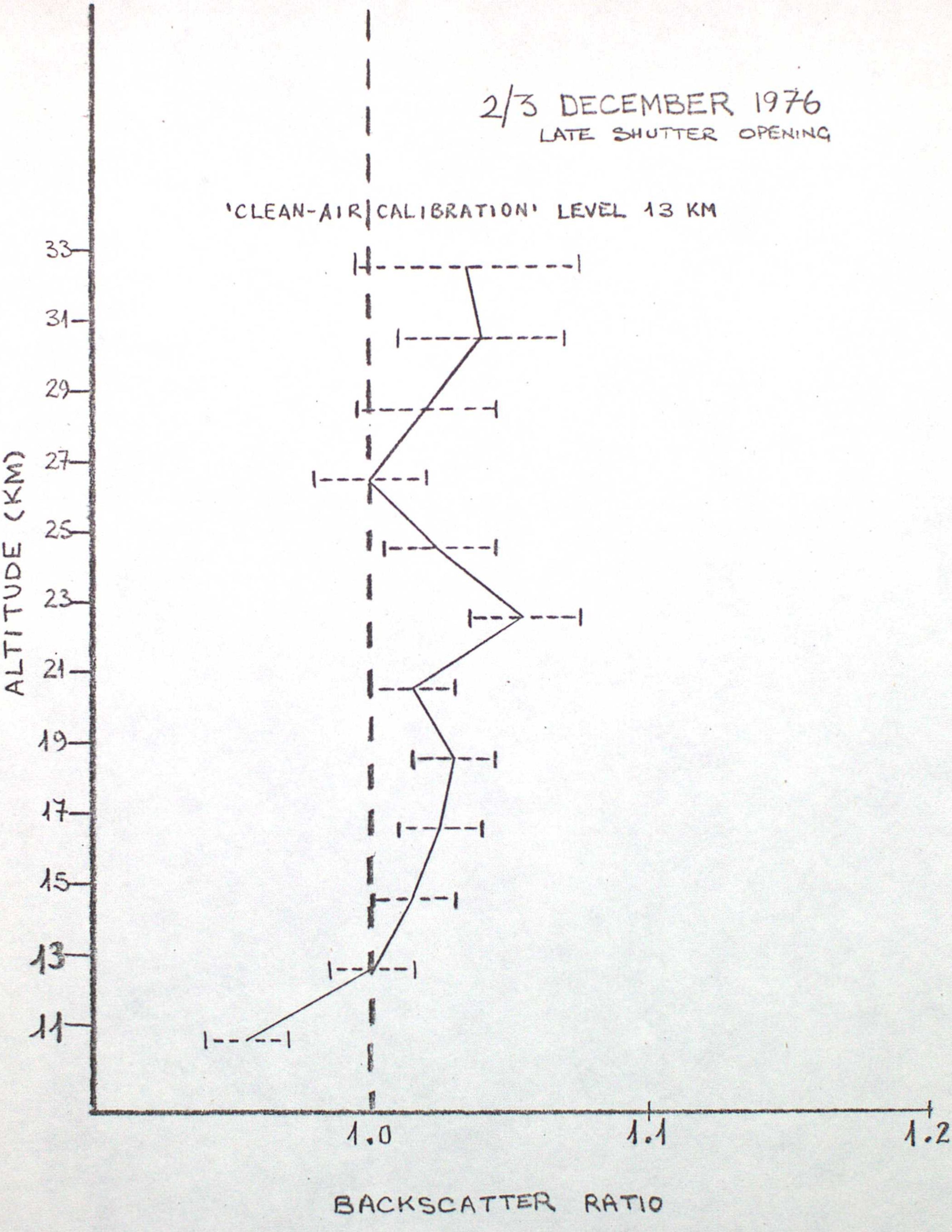

2/3 DECEMBER 1976
LATE SHUTTER OPENING
'CLEAN-AIR CALIBRATION' LEVEL 13 KM
ALTITUDE (KM)
33
31
29
27
25
23
21
19
17
15
13
11
1.0
1.1
1.2
BACKSCATTER RATIO

FIG. 8

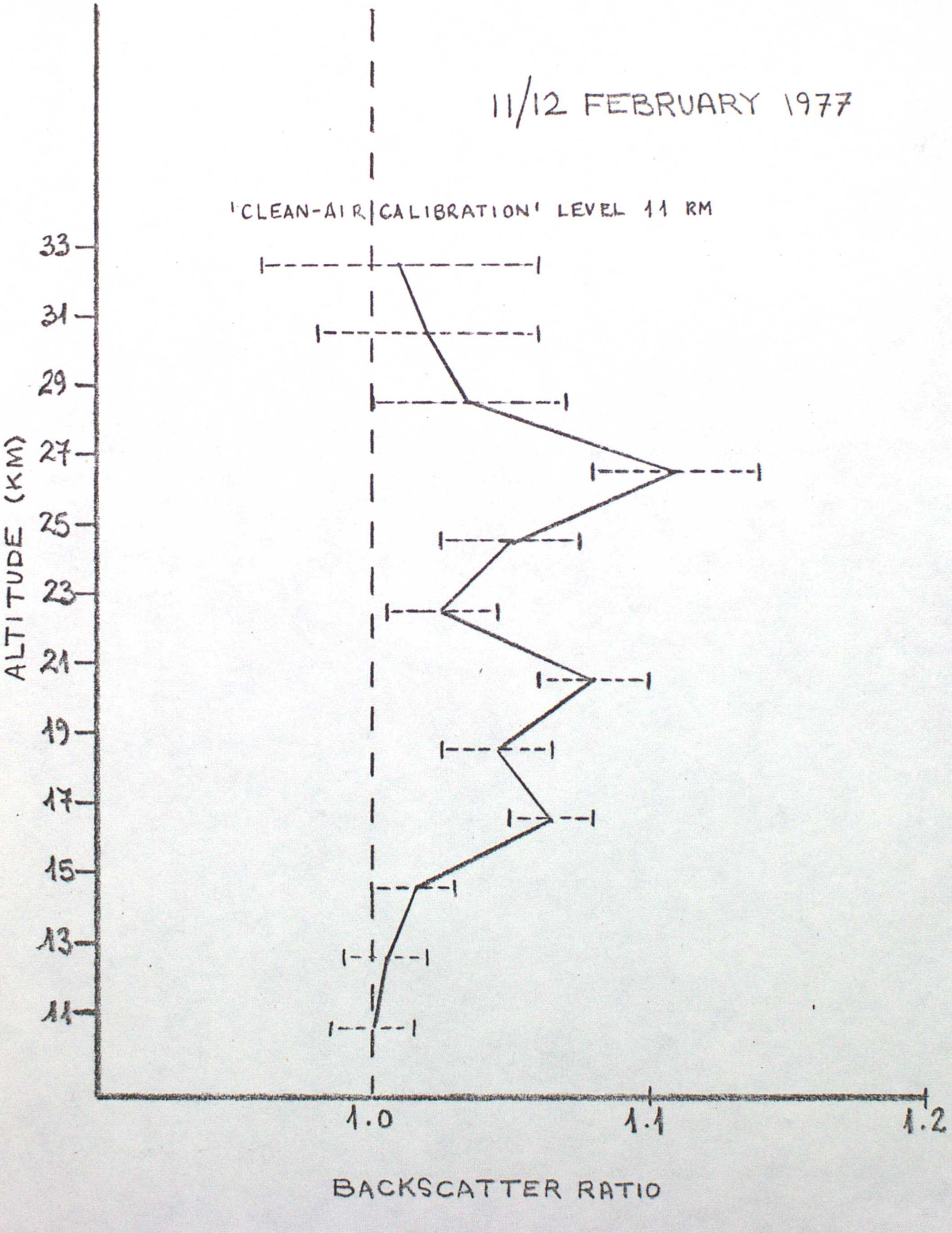

11/12 FEBRUARY 1977
'CLEAN-AIR CALIBRATION' LEVEL 11 KM
ALTITUDE (KM)
33
31
29
27
25
23
21
19
17
15
13
11
1.0
1.1
1.2
BACKSCATTER RATIO

FIG. 9

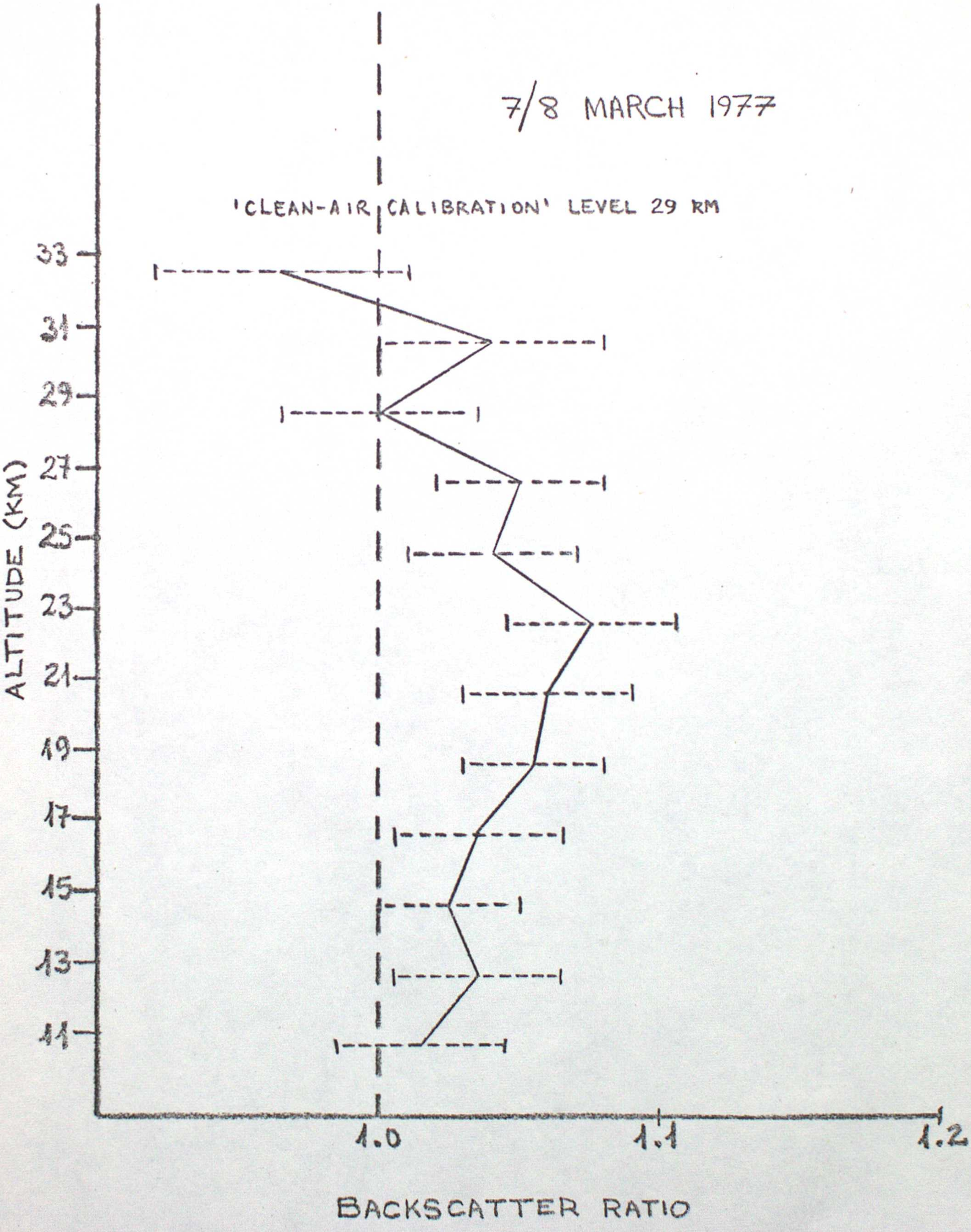
7/8 MARCH 1977
'CLEAN-AIR CALIBRATION' LEVEL 29 KM
ALTITUDE (KM)
33
31
29
27
25
23
21
19
17
15
13
11
1.0
1.1
1.2
BACKSCATTER RATIO

FIG. 10

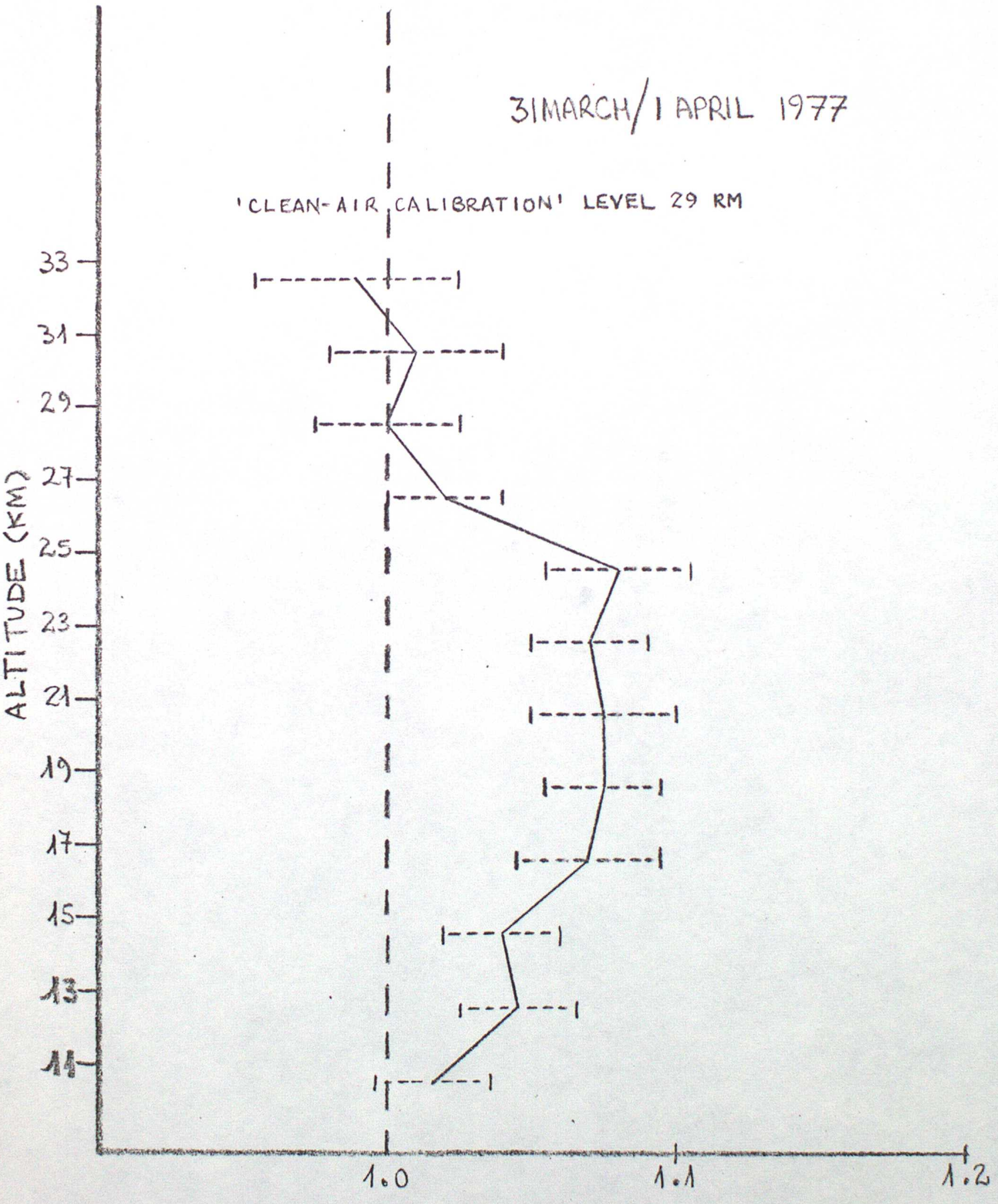

31 MARCH / 1 APRIL 1977
'CLEAN-AIR CALIBRATION' LEVEL 29 KM
ALTITUDE (KM)
33
31
29
27
25
23
21
19
17
15
13
11
1.0
1.1
1.2
BACKSCATTER RATIO

FIG. 11

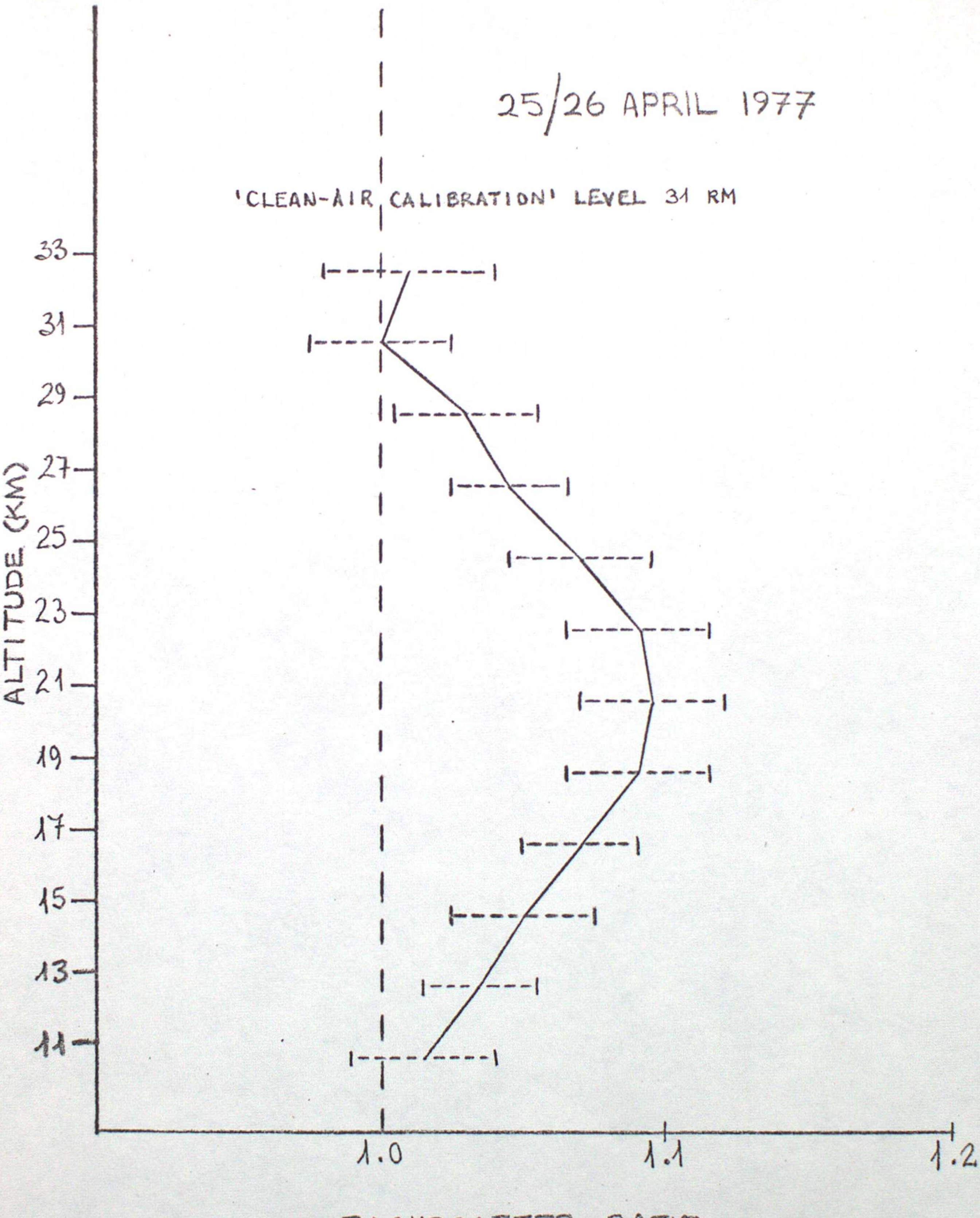
25/26 APRIL 1977
'CLEAN-AIR CALIBRATION' LEVEL 31 KM
ALTITUDE (KM)
33
31
29
27
25
23
21
19
17
15
13
11
1.0
1.1
1.2
BACKSCATTER RATIO

FIG. 12

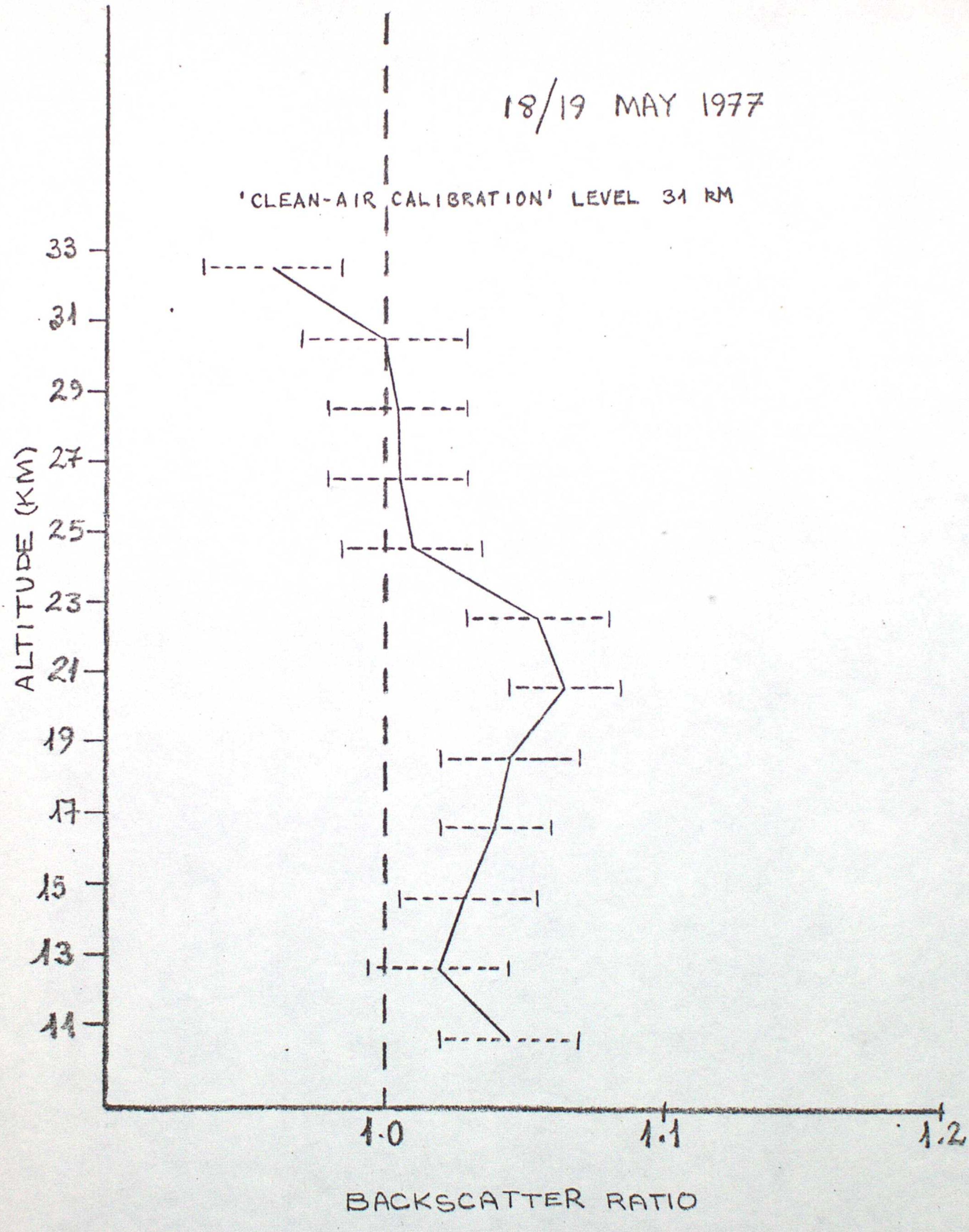
18/19 MAY 1977
'CLEAN-AIR CALIBRATION' LEVEL 31 KM
ALTITUDE (KM)
33
31
29
27
25
23
21
19
17
15
13
11
1.0
1.1
1.2
BACKSCATTER RATIO

FIG. 13

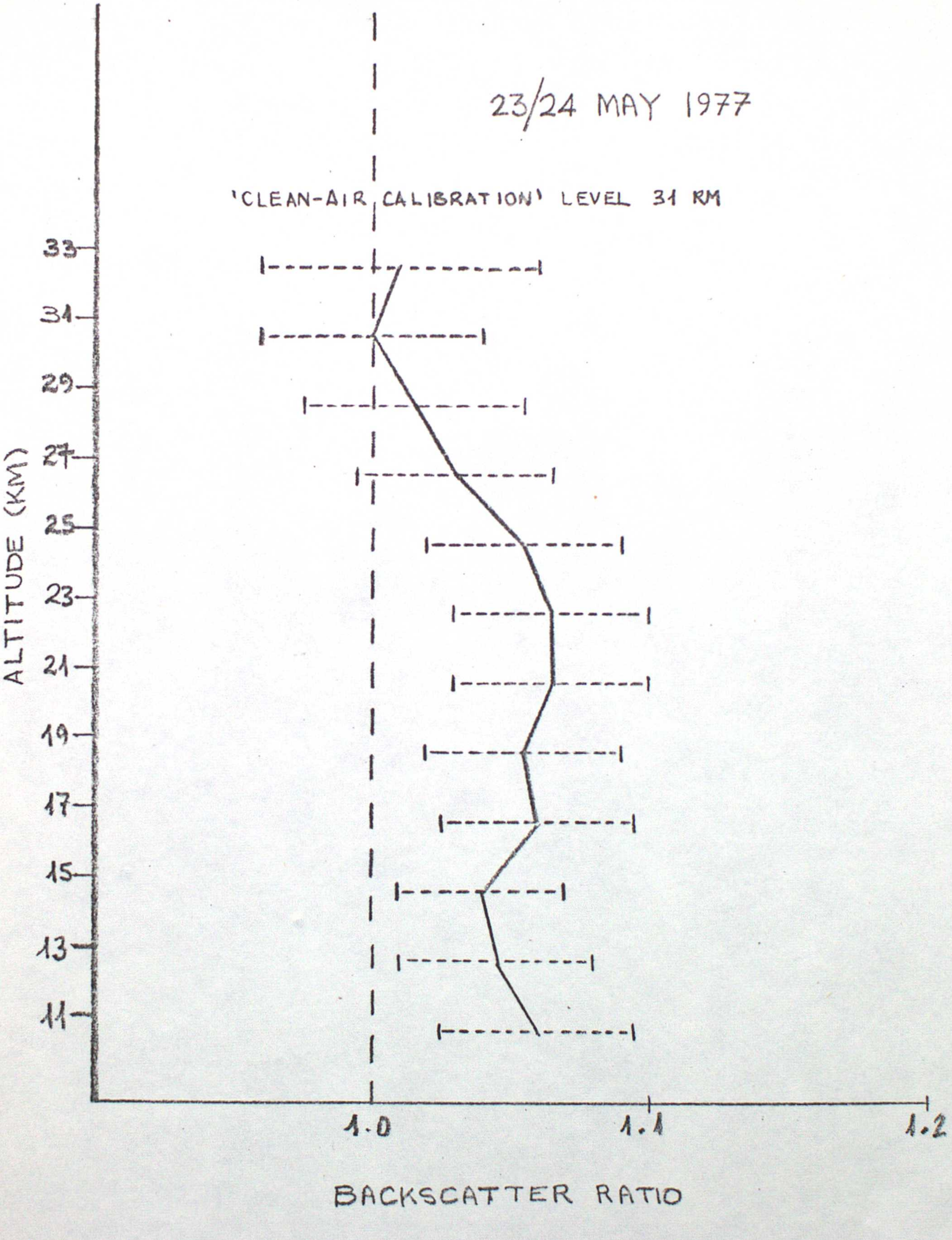
23/24 MAY 1977
'CLEAN-AIR CALIBRATION' LEVEL 31 KM
ALTITUDE (KM)
33
31
29
27
25
23
21
19
17
15
13
11
1.0
1.1
1.2
BACKSCATTER RATIO

FIG. 14

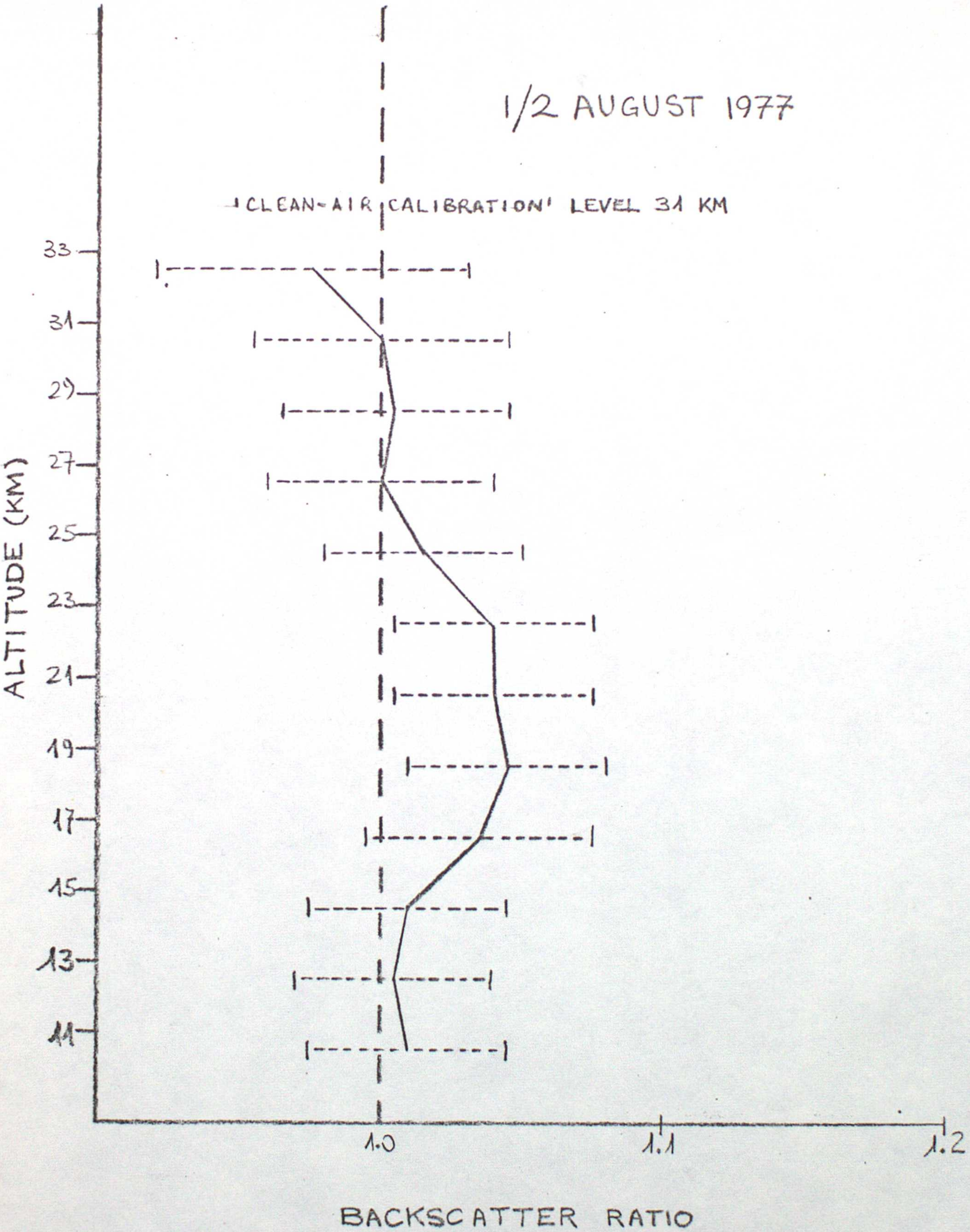
1/2 AUGUST 1977
CLEAN-AIR CALIBRATION LEVEL 31 KM
ALTITUDE (KM)
33
31
29
27
25
23
21
19
17
15
13
11
1.0
1.1
1.2
BACKSCATTER RATIO

FIG. 15

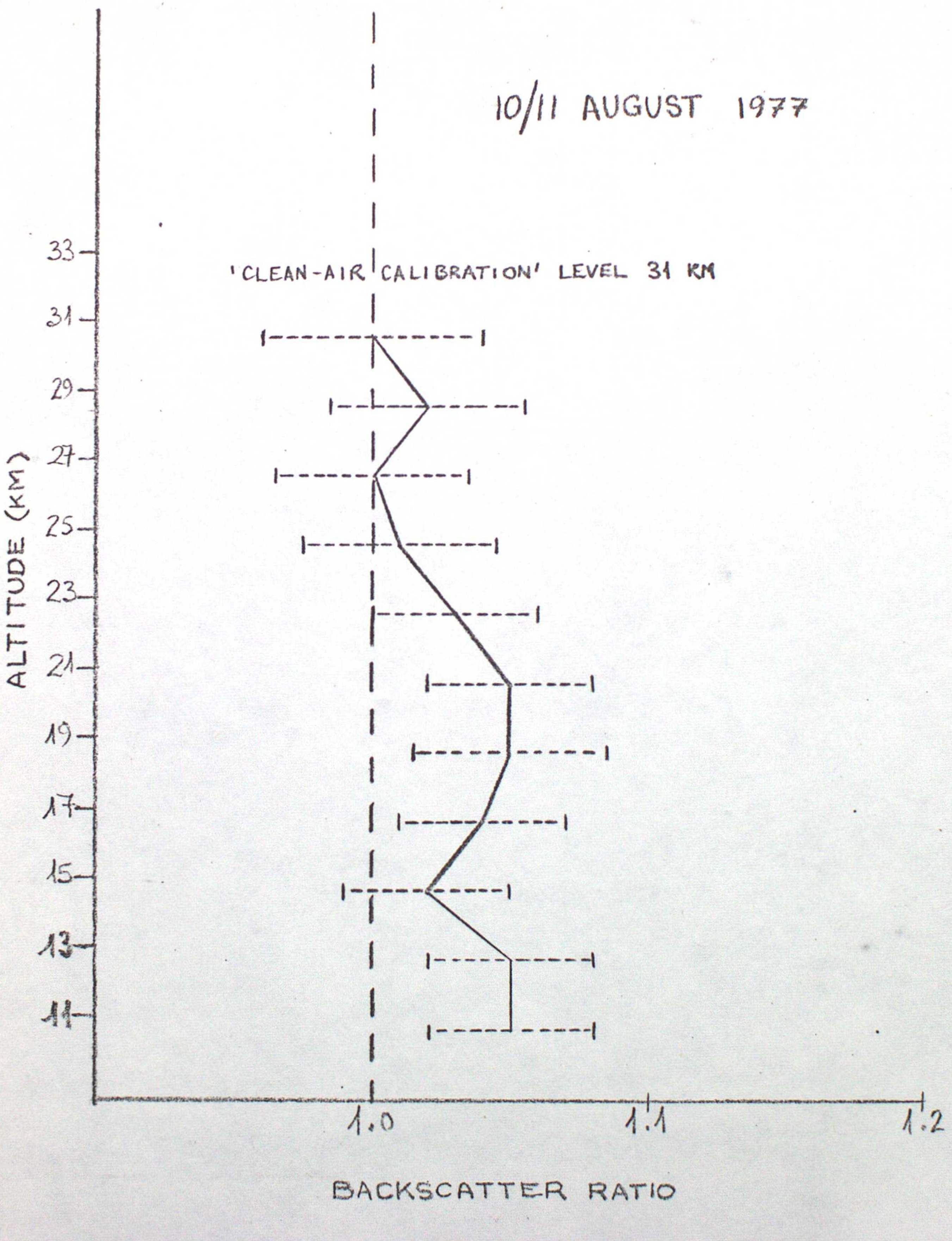
10/11 AUGUST 1977
'CLEAN-AIR CALIBRATION' LEVEL 31 KM
ALTITUDE (KM)
33
31
29
27
25
23
21
19
17
15
13
11
1.0
1.1
1.2
BACKSCATTER RATIO

FIG. 16

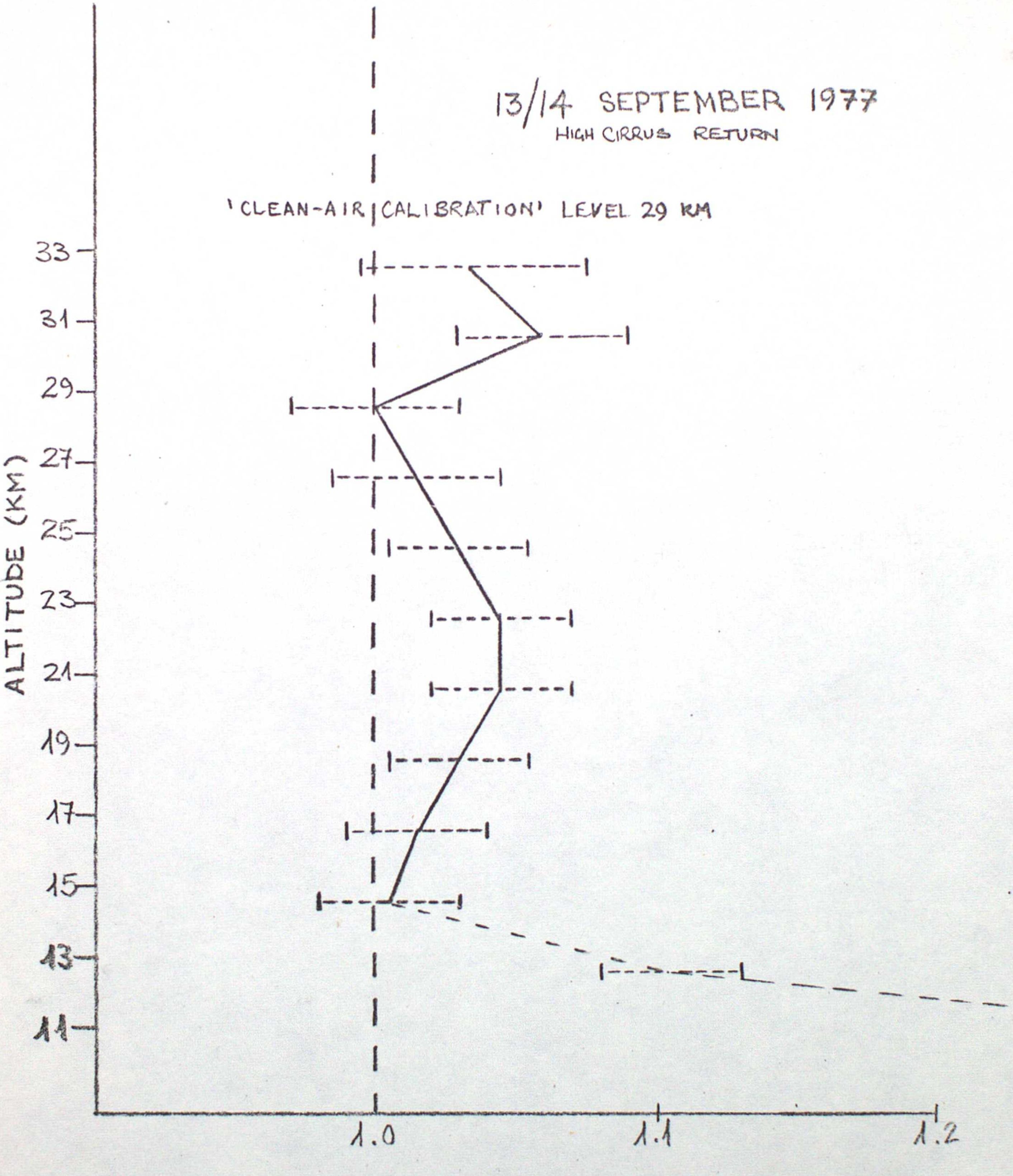
13/14 SEPTEMBER 1977
HIGH CIRRUS RETURN
'CLEAN-AIR CALIBRATION' LEVEL 29 KM
33
31
29
27
25
23
21
19
17
15
13
11
ALTITUDE (KM)
1.0
1.1
1.2
BACKSCATTER RATIO

FIG. 17

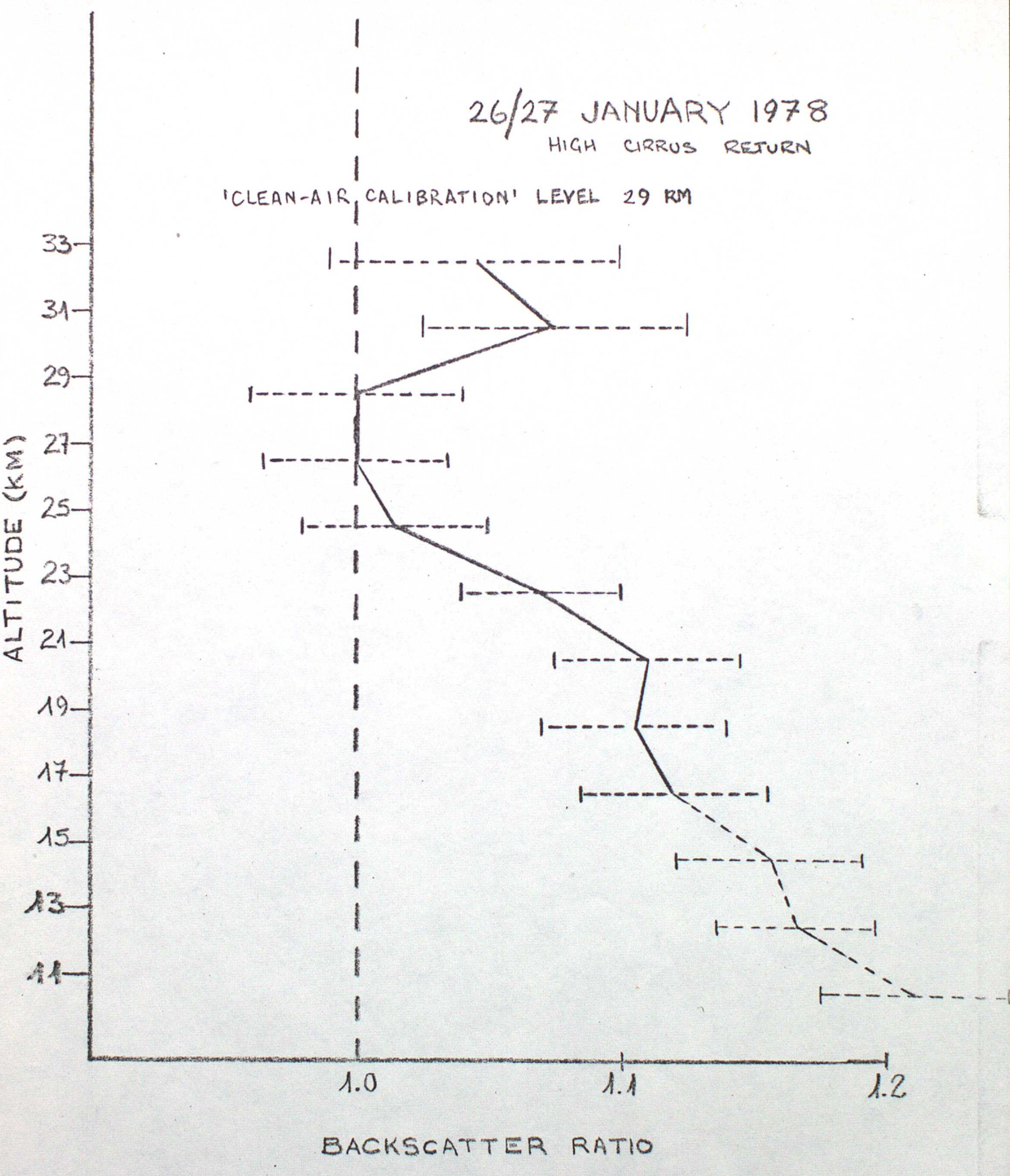
26/27 JANUARY 1978
HIGH CIRRUS RETURN
'CLEAN-AIR CALIBRATION' LEVEL 29 KM
33
31
29
27
25
23
21
19
17
15
13
11
ALTITUDE (KM)
1.0
1.1
1.2
BACKSCATTER RATIO

FIG. 18

TWO WAVELENGTH EXPERIMENT

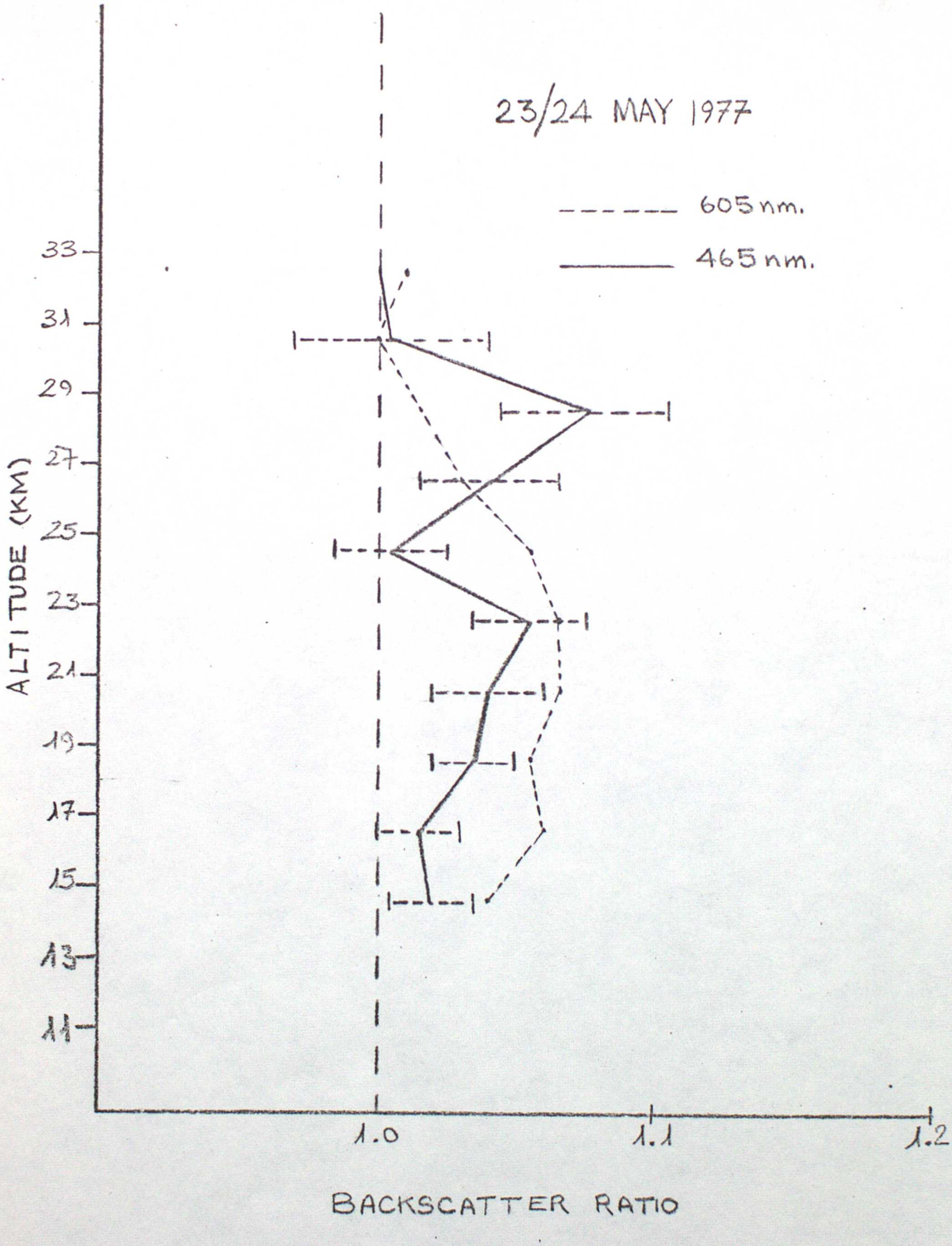

FIG. 19

AVERAGE BACKSCATTER RATIO PROFILE 1977

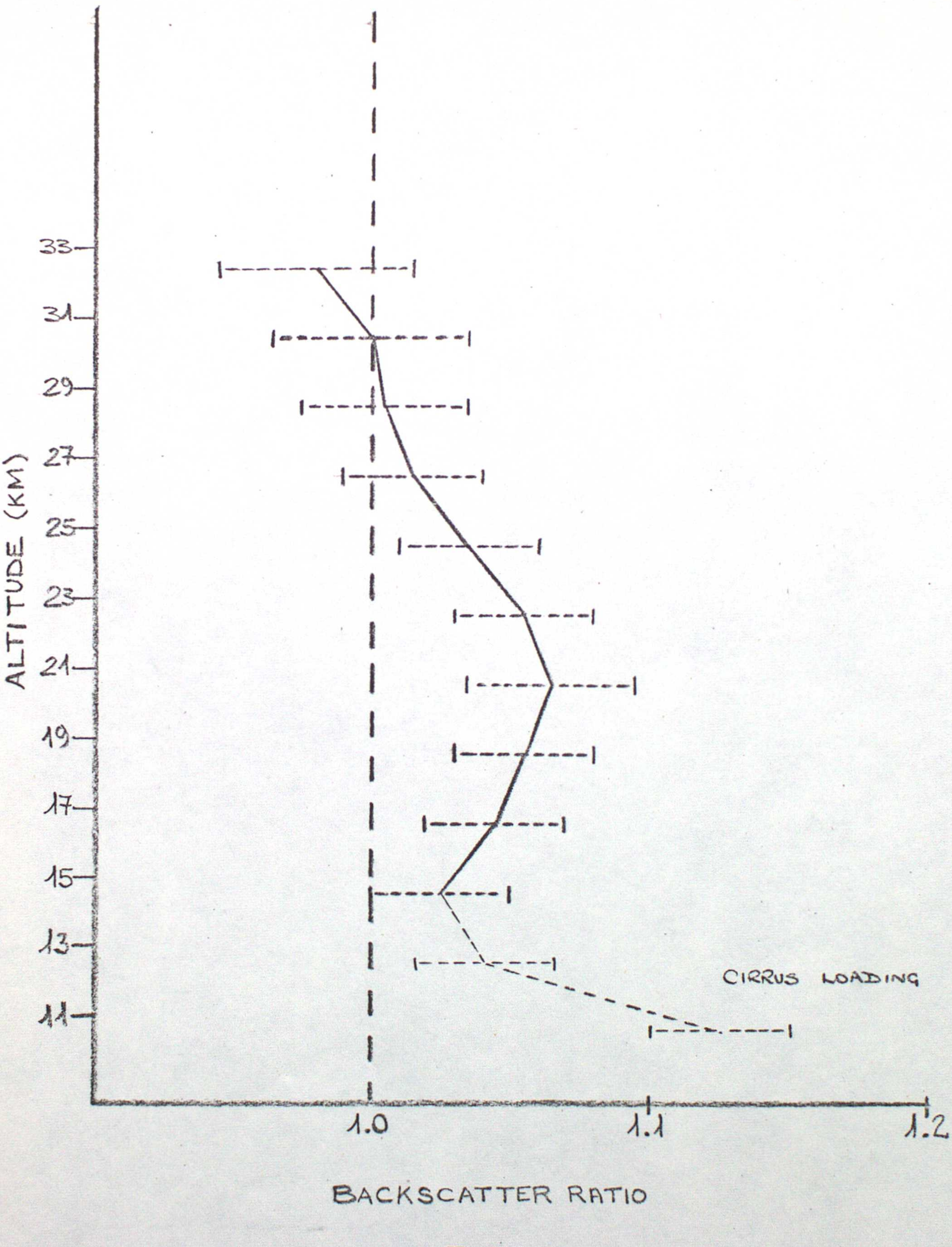

FIG. 20

COMPARISON OF HIGH AND LOW LEVEL NORMALISATION ON

PROFILE SHAPE

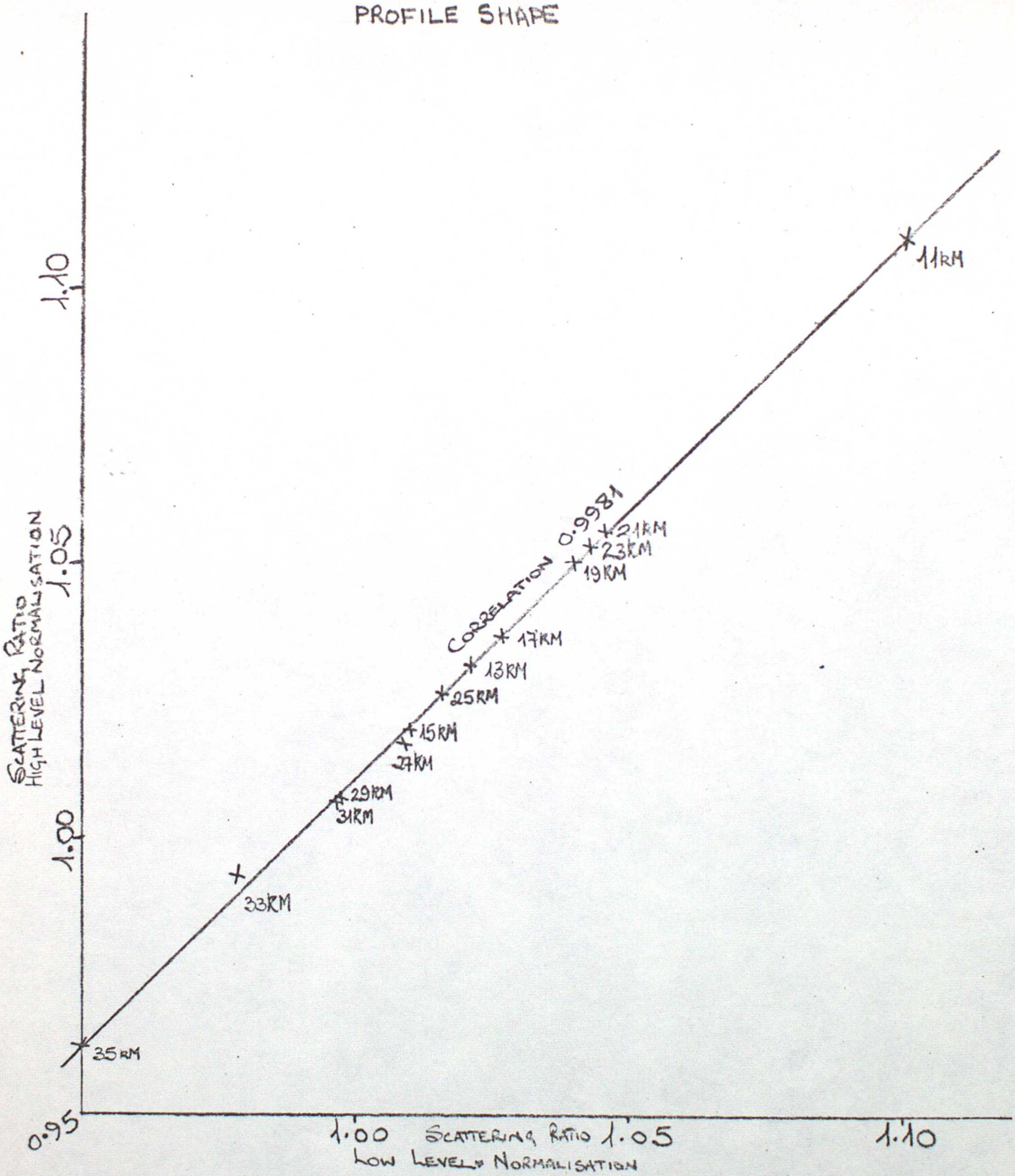

FIG. 21

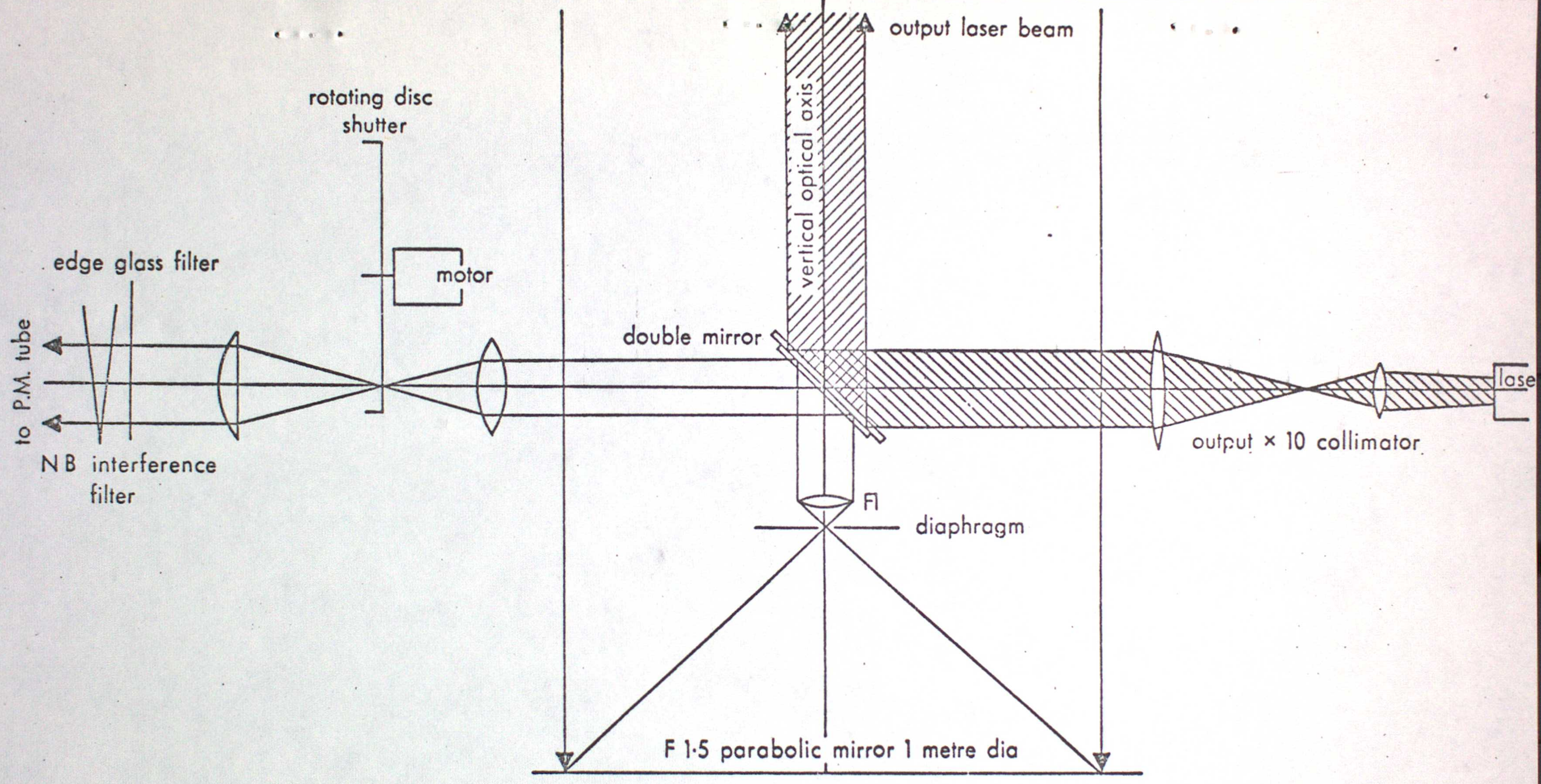

Figure 22. Schematic of the Beaufort Park Lidar

Fig. 23. Mean Backscatter Ratio 15-33km 1976-1977

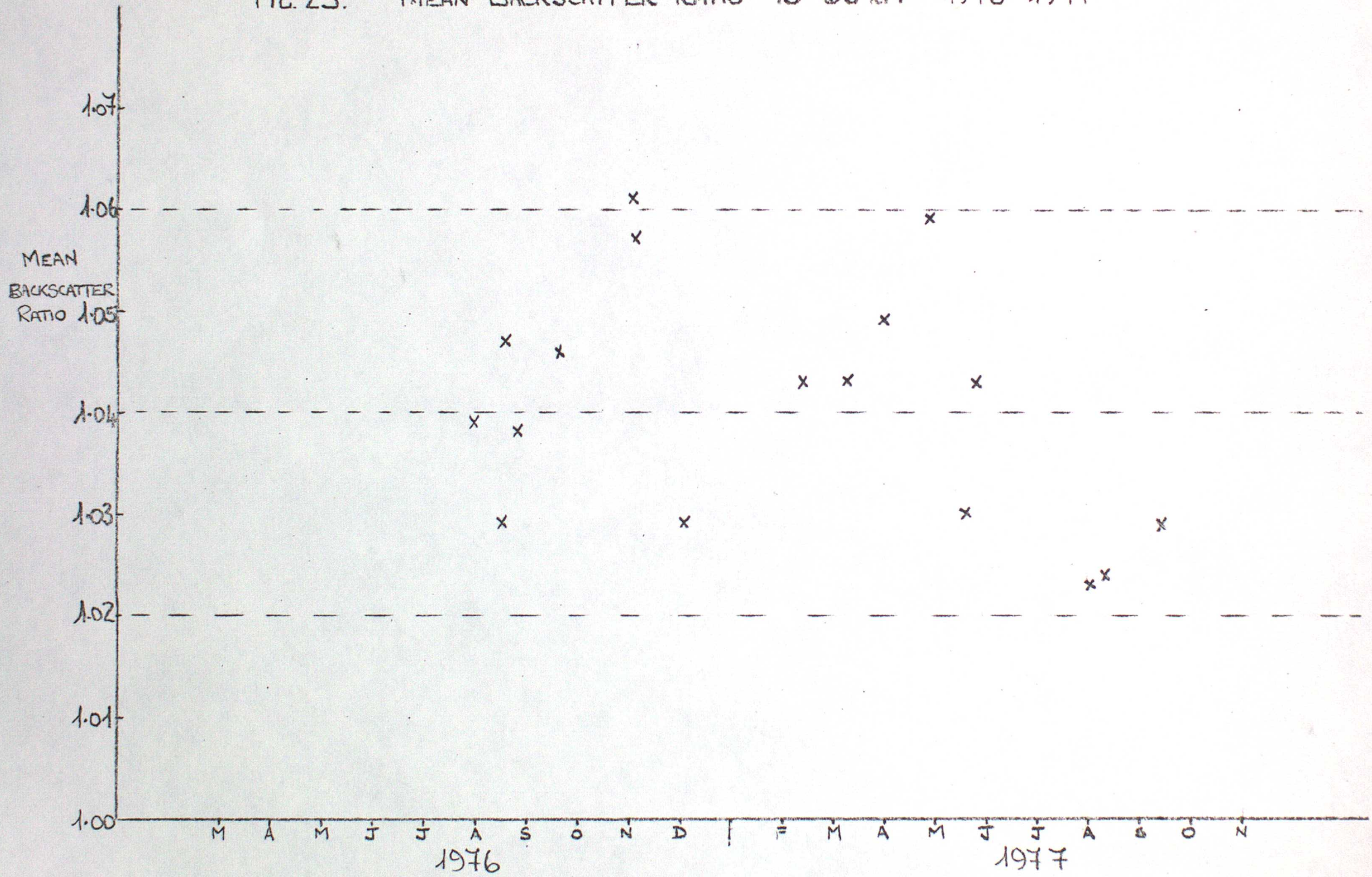

FIG. 24 PERCENTAGE CONTRIBUTION TO MEAN BACKSCATTER RATIO (MBR) 1976-1977

X = % CONTRIBUTION TO MBR BETWEEN 23 & 33 KM

⊙ = % " " " " 15 & 23 KM

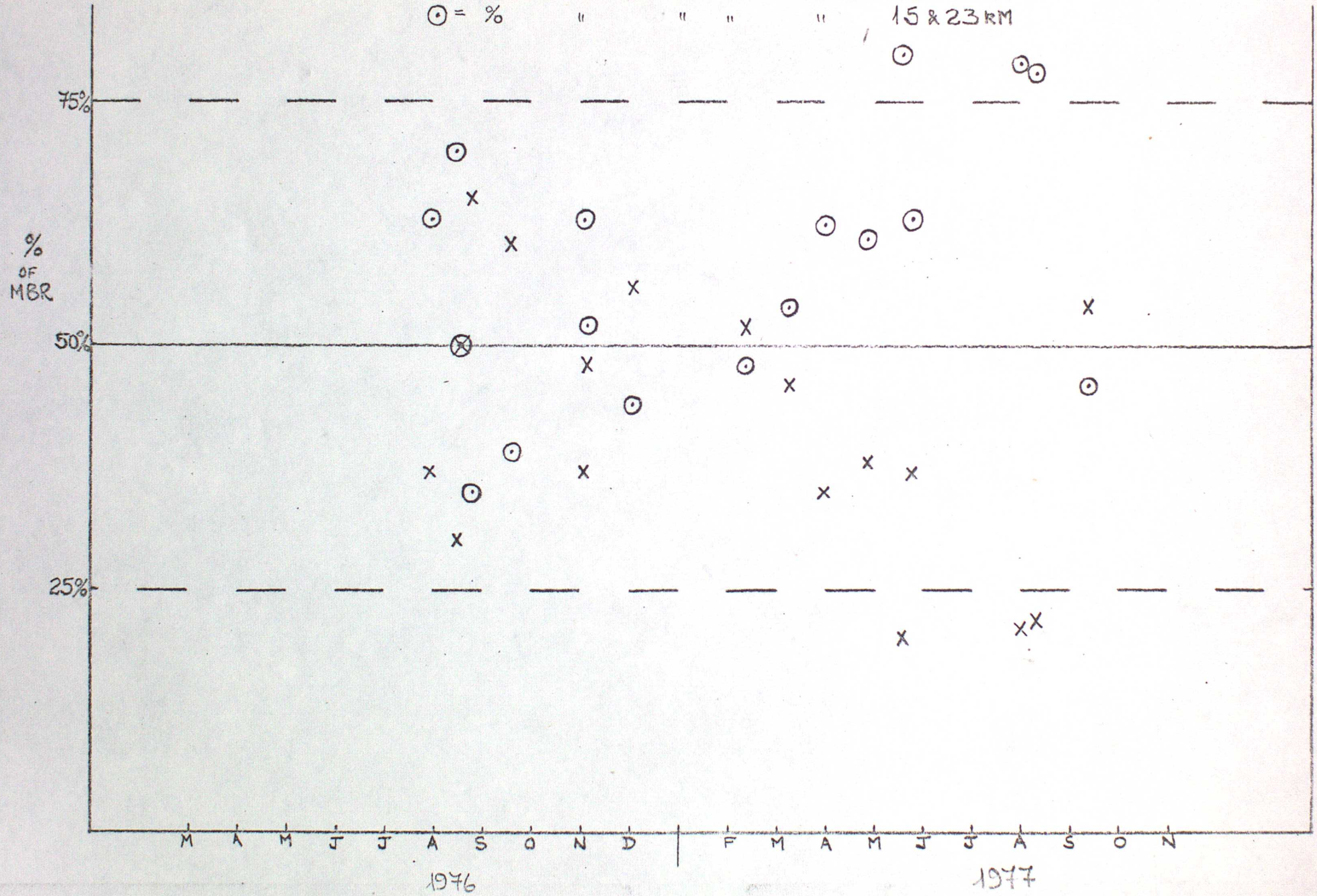

The COX-3 laser

1. Introduction

The COX-3 laser is a coaxial flashlamp pumped dye laser which has been investigated for use as a lidar transmitter. The COX-3 laser has been described in detail by Morrow and Price (1974) and consists essentially of an inner Spectrosil tube, through which the dye flows, positioned coaxially within an outer sealed Vitrosil Xenon filled flashlamp. The evaluation of this laser involved the following studies:

i. the determination of the energy output of the laser for both Rhodamine 6G and Esculin monohydrate.

ii. determination of the optimum concentration of Rhodamine 6G solution for use with the lidar receiver optics.

iii. assessment of the reliability of the laser when operated in the continuous firing mode.

2. Energy measurements

The energy measurements for R6G solutions were divided into two parts:

i. measurements of energy output with various concentrations of R6G in pure ethanol.

ii. energy measurements with various concentrations of R6G in a solution of 10% ethanol, 14% Ammonyx - LO, 76% deionized water. (This was the standard solution for use in the double-elliptical cavity (DEC) laser.)

For the range of concentrations studied the solutions of R6G in pure ethonol gave significantly larger values of energy than for the above 'standard' solution. Results for R6G in pure ethanol are summarized in Fig A1. It can be seen that output energy is approximately constant, at 150 mJ, over the range of concentrations 1.5×10^{-4} mol l^{-1} to 4.5×10^{-4} mol l^{-1}.

One of the features observed when firing continuously with solutions of R6G in pure ethanol was the production of bubbles in the lasing volume, created by the intense heat generated during the flashlamp discharge. Because of these bubbles and their possible effects on beam divergence it was decided not to investigate this lasing solution further, and concentrate instead on the above standard solution. Using this solution as the lasing medium no bubbles were observed, but unfortunately the energy output was reduced considerably, typical values being about 80 mJ over the range of concentrations used.

Measurements on solutions of Esculin monohydrate (EMH) were limited but showed promise. Only one concentration of EMH (84.0×10^{-4} mol l^{-1} in pure ethanol) was used for all measurements.

The output energy of the EMH dye depended on the size of the discharge capacitor (and hence the flash rise time) for a given input energy. In particular the 0.22 μF 35 kV capacitor when used to provide 100 joules input energy to the flashlamp gave a laser output of 120 mJ. On replacement by a 1.0 μF 25 kV capacitor the output energy for the same input energy (100 joules) was 85 mJ.

For both dyes the full width half maximum of the laser pulse was less than 0.5 μs (typically of the order of 0.4 μs).

3. Assessment of Reliability

One of the major requirements for lasers in lidar applications is the capability for rapid continuous firing ($\sim$1 per sec) sequences of several thousand shots. The COX-3 laser was tested in this way for periods of up to one hour duration at a maximum rate of 68 shots per minute with a 100 joule input. With adequate seal cooling Morrow and Price (1974) maintain that this laser is capable of 10 shots per sec.

In addition to this requirement the time 'jitter' between the trigger pulse and the laser pulse, must be within certain limits to enable the backscatter return to be recorded before the shutter closes. In this respect the COX-3 laser has shown itself to be superior to the DEC laser, there being no significant variation in the time delay between the trigger pulse and the laser pulse which means fewer pulses are lost due to time jitter.

The expected lifetime of the flashtube must be at least that of a single Junge layer run, that is about 5000 shots, for the system to be feasible. The manufacturers specify a lifetime of 10^6 shots for a 100 joule input to the COX-3 laser but it must be stated that this lifetime has not been approached in our experience. The two COX-3 lasers tested both showed a decrease in hold-off voltage and ultimately burst after being fired for not more than 10,000 shots each.

After discussion with the manufacturers two standard COX-3 flashlamps were modified by the introduction of barium getters at each end inthe ballast volume. Lifetime tests on one of these modified flashlamps have proved encouraging and although not tested to the limit of 10^6 shots it was fired for over 20,000 shots in 2 sessions and slightly over 3 hours in length without showing any signs of the above change. Thus it is to be hoped that the introduction of the barium getter has eliminated the fatigue of the outer jacket due to the release of oxygen during a discharge.

Conclusion

The COX-3 laser would provide a basis for a relatively simple compact lidar system with an output energy of 100 to 150 mJ at 605 nm being easily attainable. Because of the shorter pulse length (0.5 μs) the vertical range resolution is improved by a factor of about eight which is a desirable feature for cirrus cloud measurements.

Preliminary firings into the atmosphere with the COX-3 laser have demonstrated that return signals are large enough to enable both Junge layer type measurements and cirrus cloud investigations to be carried out.

References

Morrow, T and Price, H. T. W. 1974 "A simple reliable Co-axial dye laser system". Optics Communications, 2.